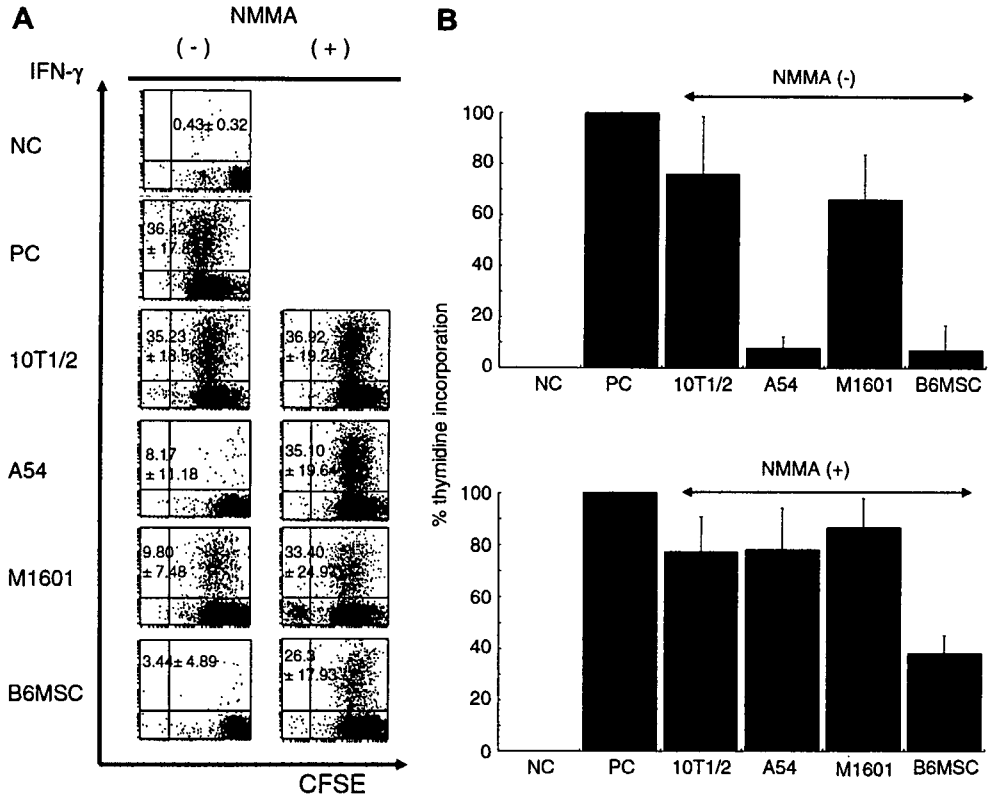

Fig. 3. A specific NO synthase inhibitor, L-NMMA, restores T cell proliferation and IFN-γ production in Th1 condition. (A) A simultaneous flow cytometric analysis of T cell differentiation and proliferation in Th1 condition as described in Fig. 1. $CD4^+$ T cells (1×10^6) were stimulated in Th1 condition in the presence of 10T1/2, A54, M1601, and primary MSCs (1×10^5) with or without 1 mM L-NMMA for 48 h. The numbers indicated are mean ± SD of the percentage of cells in upper right quadrant. (B) [^{3}H]Thymidine incorporation assay in the presence or absence of L-NMMA. $CD4^+$ T cells (1×10^5) were stimulated in Th1 condition in the presence of 10T1/2, A54, M1601, and primary MSCs (1×10^4) with or without 1 mM L-NMMA for 48 h. [^{3}H]Thymidine was pulsed for the last 6 h. 10T1/2, A54, M1601, and primary MSCs were pre-irradiated with 30 Gy to prevent [^{3}H]thymidine incorporation into MSCs. The percentage of proliferation is indicated compared to positive control, which is no MSCs. Shown are means ± SD from three independent experiments. NC, negative control; $CD4^+$ T cells alone; PC, positive control; $CD4^+$ T cells with mitogen and without MSCs.

IFN-γ and a factor that activates NF-κB are crucial for NO production from MSCs in the absence of T cells

To determine what inhibits the production of NO in Th2 condition, the two differentiation factors that mediate the Th2 pathway, anti-IFN-γ antibody and IL-4, were investigated. It is possible one or both of these factors is responsible for the minimum production of NO in Th2 condition. As shown in Fig. 4A, anti-IFN-γ antibody clearly inhibits the production of NO, whereas suppression by IL-4 was less evident. These results suggest that IFN-γ is a key regulator of NO production by MSCs.

Interestingly, cell supernatant collected from activated but not non-activated T cells had the ability to induce NO by MSCs (Supplementary Fig. 2A). What signal(s) are required for NO production by MSCs? As shown in Fig. 4A, IFN-γ is critical for NO production; however, in a T cell-free environment, IFN-γ alone does not induce production of NO from primary MSCs (Fig. 4B, both panels). IFN-γ in combination with LPS, but not IL-2, stimulates NO secretion from primary MSCs (Fig. 4B, left panel and data not shown), suggesting that both the IFN-γ and the signal from Toll-like receptor-4 (TLR4) are required for NO induction by MSCs. Could other TLR ligands substitute for LPS? The addition of flagellin induced NO production in combination with IFN-γ (Fig. 4B, left panel). While, synthetic double strand RNA, poly(I:C), and CpG-oligonucleotide did not induce NO (data not shown). Flagellin is a protein component of bacteria known to induce NO production from macrophages via TLR5 in the presence of either a TLR4 or IFN-γ signal [21,22]. In addition to these factors, IL-1β and TNF-α induce NO when provided in combination with IFN-γ (Fig. 4B, right panel and Supplementary Fig. 2B). As NF-κB is a downstream target of the signaling cascades activated by LPS, flagellin, IL-1β, and TNF-α, we hypothesized that activation of NF-κB is required for NO induction by MSCs. As shown in Fig. 4C, Bay 11-7085 [20], a specific inhibitor of NF-κB suppressed production of inducible NO synthase (iNOS) in MSCs, thus suggesting that NF-κB is involved in NO production by MSCs as well as IFN-γ.

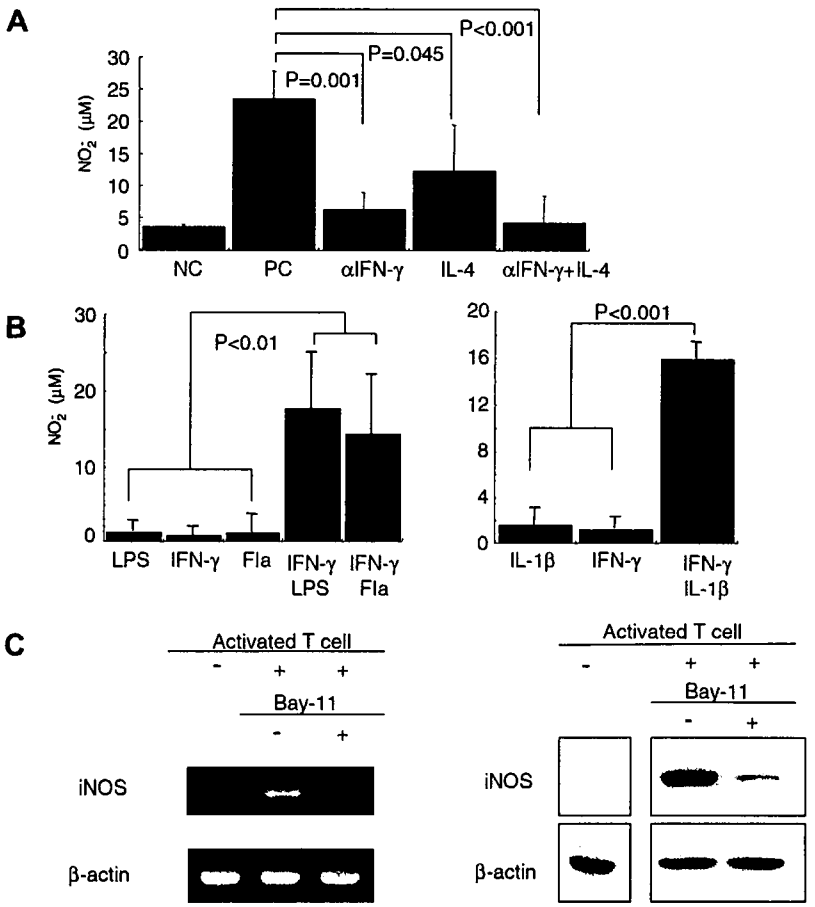

Fig. 4. IFN-γ and NF-κB are involved in NO production. (A) Anti-IFN-γ antibody inhibits NO production. $CD4^+$ T cells (1×10^6) were stimulated with anti-CD3/CD28 beads in the presence of primary MSCs (1×10^5) without any differentiation factors. A neutralizing antibody against IFN-γ (10 μg/ml), IL-4 (100 ng/ml), and a combination of both were added. NC, negative control; $CD4^+$ T cells alone; PC, positive control; $CD4^+$ T cells with mitogen. (B) LPS, flagellin, TNF-α, or IL-1β in a combination with IFN-γ induces NO production from primary MSCs in a T cell-free system. The primary MSCs (1×10^5) were treated with the indicated stimuli without T cells for 48 h and NO concentrations of supernatants were determined by the Greiss assay. (C) A NF-κB inhibitor, Bay11-7085, suppresses iNOS induction in MSCs. Unfractionated splenocytes (1×10^7) were stimulated with anti-CD3/CD28 beads for 48 h and put onto primary MSCs (1×10^6). After co-cultivation for 6 h, total RNA was harvested for RT-PCR and after 30 h, cell lysates were harvested for immunoblot analysis. In advance of co-cultivation, primary MSCs were pre-treated for 30 min with the irreversible NF-κB inhibitor, Bay11-7085 (5 μM), and washed twice with PBS. Just before harvesting, T cells were washed out extensively with PBS.

Discussion

This study demonstrates that mouse primary MSCs strongly suppress T cell proliferation and differentiation in Th1 condition, while the suppression in Th2 condition is weak. Moreover, it provided the first evidence, that NO production can elucidate the differential suppression in Th1/Th2 differentiation. We found a higher NO production in Th1 in comparison to Th2. Furthermore, L-NMMA, a specific inhibitor of NO synthases, restores not only T cell proliferation but also IFN-γ production in Th1 condition. In addition, the treatment with an anti-IFN-γ antibody resulted in a low level of NO production, suggesting that IFN-γ is critical for NO production. While the combination of IFN-γ and a NF-κB activating factor induces NO in a T cell-free system, and moreover, an inhibitor of NF-κB diminishes the induction of iNOS in MSCs, suggesting that NF-κB is also crucial for NO production by MSCs.

The suppression of IFN-γ production may be due to the suppression of cell proliferation, since differentiation is dependent upon cell division [23]. In fact, Fig. 1A, right panel shows that only proliferating cells can produce IFN-γ. However, MSCs were shown to suppress IFN-γ production, regardless of cell division [2,19].

Primary human MSCs induced a fivefold increase in IL-4 synthesis in Th2 condition [4], however, in this study, primary mouse MSCs in the Th2 pathway suppressed production of IL-4 as measured by intracellular staining and ELISA. The discrepancy may be due to species-specific difference. MSC-like cell lines also showed suppression in IL-4 production.

Our results demonstrate that LPS, flagellin, TNF-α, and IL-1β can induce NO from MSCs in a combination with

IFN-γ. These ligands are reported to induce NO from monocytes or macrophages in the presence of IFN-γ [24–28]. Monocytes and macrophages have been assumed to be prominent sources of NO. This implies, MSCs have several features in common with monocytes and macrophages. However, a combination of IFN-γ with IL-2 [27], flagellin alone [21], LPS alone [29], and IFN-γ alone [27], which induce NO from macrophages, do not induce NO from MSCs under the conditions we tested here, suggesting that MSCs also have features that make them different from monocytes and macrophages.

What is the factor required for NO induction in combination with IFN-γ? Cell supernatant from activated T cells induces NO, thus suggesting that activated T cells produce the NO inducer. Neither a soluble TNF-α receptor, a naturally occurring decoy receptor, nor a neutralizing antibody against IL-1β diminished NO production (data not shown). Our results do not define the factor from T cells but they do suggest that the factor may be a ligand that activates NF-κB in MSCs, such as LPS, flagellin, TNF-α or IL-1β.

This study demonstrate that NO is responsible for the preferential suppression of T cell proliferation in Th1 condition by MSCs, and that IFN-γ and NF-κB are involved in NO production in primary MSCs. This appears to be the first study to elucidate the molecular mechanism for preferential Th1 suppression by MSCs. Therefore, these results are considered to enhance the understanding and investigation in this field.

Acknowledgments

This work was supported in part by grants from the Ministry of Health, Welfare, and Labor of Japan and Grants-in-Aid for Scientific Research from the Ministry of Education, Science, Sports, and Technology of Japan. We also like to thank Dr. Motohiro Matsuura (Jichi Medical University) for providing flagellin, CpG, and poly(I:C).

Appendix A. Supplementary data

Supplementary data associated with this article can be found, in the online version, at doi:10.1016/j.bbrc.2007.02.054.

References

[1] B. Maitra, E. Szekely, K. Gjini, M.J. Laughlin, J. Dennis, S.E. Haynesworth, O.N. Koc, Human mesenchymal stem cells support unrelated donor hematopoietic stem cells and suppress T-cell activation, Bone Marrow Transplant. 33 (6) (2004) 597–604.

[2] S. Glennie, I. Soeiro, P.J. Dyson, E.W. Lam, F. Dazzi, Bone marrow mesenchymal stem cells induce division arrest anergy of activated T cells, Blood 105 (7) (2005) 2821–2827.

[3] M. Krampera, S. Glennie, J. Dyson, D. Scott, R. Laylor, E. Simpson, F. Dazzi, Bone marrow mesenchymal stem cells inhibit the response of naive and memory antigen-specific T cells to their cognate peptide, Blood 101 (9) (2003) 3722–3729.

[4] S. Aggarwal, M.F. Pittenger, Human mesenchymal stem cells modulate allogeneic immune cell responses, Blood 105 (4) (2005) 1815–1822.

[5] M. Krampera, L. Cosmi, R. Angeli, A. Pasini, F. Liotta, A. Andreini, V. Santarlasci, B. Mazzinghi, G. Pizzolo, F. Vinante, P. Romagnani, E. Maggi, S. Romagnani, F. Annunziato, Role for interferon-gamma in the immunomodulatory activity of human bone marrow mesenchymal stem cells, Stem Cells 24 (2) (2006) 386–398.

[6] E. Zappia, S. Casazza, E. Pedemonte, F. Benvenuto, I. Bonanni, E. Gerdoni, D. Giunti, A. Ceravolo, F. Cazzanti, F. Frassoni, G. Mancardi, A. Uccelli, Mesenchymal stem cells ameliorate experimental autoimmune encephalomyelitis inducing T-cell anergy, Blood 106 (5) (2005) 1755–1761.

[7] J. Matsuzaki, T. Tsuji, I. Imazeki, H. Ikeda, T. Nishimura, Immunosteroid as a regulator for Th1/Th2 balance: its possible role in autoimmune diseases, Autoimmunity 38 (5) (2005) 369–375.

[8] V.M. Hubbard, J.M. Eng, T. Ramirez-Montagut, K.H. Tjoe, S.J. Muriglan, A.A. Kochman, T.H. Terwey, L.M. Willis, R. Schiro, G. Heller, G.F. Murphy, C. Liu, O. Alpdogan, M.R. van den Brink, Absence of inducible costimulator on alloreactive T cells reduces graft versus host disease and induces Th2 deviation, Blood 106 (9) (2005) 3285–3292.

[9] M. Nishikawa, K. Ozawa, A. Tojo, T. Yoshikubo, A. Okano, K. Tani, K. Ikebuchi, H. Nakauchi, S. Asano, Changes in hematopoiesis-supporting ability of C3H10T1/2 mouse embryo fibroblasts during differentiation, Blood 81 (5) (1993) 1184–1192.

[10] F. Djouad, P. Plence, C. Bony, P. Tropel, F. Apparailly, J. Sany, D. Noel, C. Jorgensen, Immunosuppressive effect of mesenchymal stem cells favors tumor growth in allogeneic animals, Blood 102 (10) (2003) 3837–3844.

[11] H. Sowa, H. Kaji, L. Canaff, G.N. Hendy, T. Tsukamoto, T. Yamaguchi, K. Miyazono, T. Sugimoto, K. Chihara, Inactivation of menin, the product of the multiple endocrine neoplasia type 1 gene, inhibits the commitment of multipotential mesenchymal stem cells into the osteoblast lineage, J. Biol. Chem. 278 (23) (2003) 21058–21069.

[12] B.L. Atkinson, K.S. Fantle, J.J. Benedict, W.E. Huffer, A. Gutierrez-Hartmann, Combination of osteoinductive one proteins differentiates mesenchymal C3H/10T1/2 cells specifically to the cartilage lineage, J. Cell. Biochem. 65 (3) (1997) 325–339.

[13] D. Gazit, R. Ebner, A.J. Kahn, R. Derynck, Modulation of expression and cell surface binding of members of the transforming growth factor-beta superfamily during retinoic acid-induced osteoblastic differentiation of multipotential mesenchymal cells, Mol. Endocrinol. 7 (2) (1993) 189–198.

[14] C.M. Shea, C.M. Edgar, T.A. Einhorn, L.C. Gerstenfeld, BMP treatment of C3H10T1/2 mesenchymal stem cells induces both chondrogenesis and osteogenesis, J. Cell. Biochem. 90 (6) (2003) 1112–1127.

[15] J.E. Albina, J.A. Abate, W.L. Henry Jr., Nitric oxide production is required for murine resident peritoneal macrophages to suppress mitogen-stimulated T cell proliferation. Role of IFN-gamma in the induction of the nitric oxide-synthesizing pathway, J. Immunol. 147 (1) (1991) 144–148.

[16] R.M. Bingisser, P.A. Tilbrook, P.G. Holt, U.R. Kees, Macrophage-derived nitric oxide regulates T cell activation via reversible disruption of the Jak3/STAT5 signaling pathway, J. Immunol. 160 (12) (1998) 5729–5734.

[17] R.C. van der Veen, T.A. Dietlin, L. Pen, J.D. Gray, F.M. Hofman, Antigen presentation to Th1 but not Th2 cells by macrophages results in nitric oxide production and inhibition of T cell proliferation: interferon-gamma is essential but insufficient, Cell. Immunol. 206 (2) (2000) 125–135.

[18] R.C. van der Veen, T.A. Dietlin, J. Dixon Gray, W. Gilmore, Macrophage-derived nitric oxide inhibits the proliferation of activated T helper cells and is induced during antigenic stimulation of resting T cells, Cell. Immunol. 199 (1) (2000) 43–49.

[19] K. Sato, K. Ozaki, I. Oh, A. Meguro, K. Hatanaka, T. Nagai, K. Muroi, K. Ozawa, Nitric oxide plays a critical role in suppression of T-cell proliferation by mesenchymal stem cells, Blood 109 (1) (2007) 228–234.

[20] J.W. Pierce, R. Schoenleber, G. Jesmok, J. Best, S.A. Moore, T. Collins, M.E. Gerritsen, Novel inhibitors of cytokine-induced IκBα phosphorylation and endothelial cell adhesion molecule expression show anti-inflammatory effects in vivo, J. Biol. Chem. 272 (34) (1997) 21096–21103.

[21] S.B. Mizel, A.N. Honko, M.A. Moors, P.S. Smith, A.P. West, Induction of macrophage nitric oxide production by Gram-negative flagellin involves signaling via heteromeric Toll-like receptor 5/Toll-like receptor 4 complexes, J. Immunol. 170 (12) (2003) 6217–6223.

[22] M.A. Moors, L. Li, S.B. Mizel, Activation of interleukin-1 receptor-associated kinase by gram-negative flagellin, Infect. Immun. 69 (7) (2001) 4424–4429.

[23] J.J. Bird, D.R. Brown, A.C. Mullen, N.H. Moskowitz, M.A. Mahowald, J.R. Sider, T.F. Gajewski, C.R. Wang, S.L. Reiner, Helper T cell differentiation is controlled by the cell cycle, Immunity 9 (2) (1998) 229–237.

[24] R.B. Lorsbach, W.J. Murphy, C.J. Lowenstein, S.H. Snyder, S.W. Russell, Expression of the nitric oxide synthase gene in mouse macrophages activated for tumor cell killing. Molecular basis for the synergy between interferon-gamma and lipopolysaccharide, J. Biol. Chem. 268 (3) (1993) 1908–1913.

[25] R. Brewington, M. Chatterji, M. Zoubine, R.N. Miranda, M. Norimatsu, A. Shnyra, IFN-gamma-independent autocrine cytokine regulatory mechanism in reprogramming of macrophage responses to bacterial lipopolysaccharide, J. Immunol. 167 (1) (2001) 392–398.

[26] M.A. Munoz-Fernandez, M.A. Fernandez, M. Fresno, Synergism between tumor necrosis factor-alpha and interferon-gamma on macrophage activation for the killing of intracellular Trypanosoma cruzi through a nitric oxide-dependent mechanism, Eur. J. Immunol. 22 (2) (1992) 301–307.

[27] W. Deng, B. Thiel, C.S. Tannenbaum, T.A. Hamilton, D.J. Stuehr, Synergistic cooperation between T cell lymphokines for induction of the nitric oxide synthase gene in murine peritoneal macrophages, J. Immunol. 151 (1) (1993) 322–329.

[28] M. Bose, P. Farnia, Proinflammatory cytokines can significantly induce human mononuclear phagocytes to produce nitric oxide by a cell maturation-dependent process, Immunol. Lett. 48 (1) (1995) 59–64.

[29] S. Yoshida, Y.H. Lee, M. Hassan, T. Shoji, K. Onuma, H. Hasegawa, H. Nakagawa, S. Serizawa, H. Amayasu, Parallel induction of nitric oxide and tetrahydrobiopterin synthesis in alveolar macrophages, Respiration 68 (3) (2001) 299–306.

Nitric oxide plays a critical role in suppression of T-cell proliferation by mesenchymal stem cells

Kazuya Sato,[1] Katsutoshi Ozaki,[1] Iekuni Oh,[1] Akiko Meguro,[1] Keiko Hatanaka,[1] Tadashi Nagai,[1] Kazuo Muroi,[1] and Keiya Ozawa[1]

[1]Division of Hematology, Jichi Medical University, Tochigi, Japan

The molecular mechanisms by which mesenchymal stem cells (MSCs) suppress T-cell proliferation are poorly understood, and whether a soluble factor plays a major role remains controversial. Here we demonstrate that the T-cell–receptor complex is not a target for the suppression, suggesting that downstream signals mediate the suppression. We found that Stat5 phosphorylation in T cells is suppressed in the presence of MSCs and that nitric oxide (NO) is involved in the suppression of Stat5 phosphorylation and T-cell proliferation. The induction of inducible NO synthase (NOS) was readily detected in MSCs but not T cells, and a specific inhibitor of NOS reversed the suppression of Stat5 phosphorylation and T-cell proliferation. This production of NO in the presence of MSCs was mediated by CD4 or CD8 T cells but not by CD19 B cells. Furthermore, inhibitors of prostaglandin synthase or NOS restored the proliferation of T cells, whereas an inhibitor of indoleamine 2,3-dioxygenase and a transforming growth factor–β–neutralizing antibody had no effect. Finally, MSCs from inducible NOS$^{-/-}$ mice had a reduced ability to suppress T-cell proliferation. Taken together, these results suggest that NO produced by MSCs is one of the major mediators of T-cell suppression by MSCs. (Blood. 2007;109:228-234)

Introduction

Because mesenchymal stem cells (MSCs) differentiate into osteocytes, chondrocytes, myotubes, and adipocytes,[1-3] they are expected to become a source of cells for regenerative therapy. Also, MSCs support hematopoietic stem cell engraftment[4-9] and modulate immunologic responses by unknown mechanisms.[9-14] Here, we investigated the molecular mechanisms by which MSCs suppress T-cell proliferation.

Transforming growth factor–β (TGF-β), hepatocyte growth factor, indoleamine 2,3-dioxygenase (IDO), and prostaglandin E2 (PGE_2) have been reported to mediate T-cell suppression by MSCs.[13-15] Specifically, neutralizing antibodies against TGF-β or hepatocyte growth factor,[13] an inhibitor of IDO,[14] or an inhibitor of prostaglandin production reverse the inhibition of T-cell proliferation by MSCs.[15] In addition, some reports have shown that a soluble factor is the major mediator of suppression,[13-17] whereas some reports have demonstrated that T-cell–MSC contact is required for this suppression.[12-14,16,17] In the current study, we sought to resolve these conflicting results by using a mouse bone marrow–derived MSC system.

One candidate soluble factor for T-cell suppression is nitric oxide (NO) because it is known to inhibit T-cell proliferation.[18-25] NO is produced by NO synthases (NOSs), of which there are 3 subtypes: inducible NOS (iNOS), endothelial NOS, and neuronal NOS. Like MSCs, it has been known that macrophages suppress T-cell proliferation. This suppression was reported to be mediated by NO inhibition of Stat5 phosphorylation.[18,19] Also, MSCs were reported to produce NO when they differentiate into chondrocytes.[26] We therefore investigated whether MSCs can produce NO and whether NO is involved in their ability to suppress T-cell proliferation.

Materials and methods

Materials

N-nitro-L-arginine methyl ester (L-NAME), indomethacin, and concanavalin A (Con A) were purchased from Wako (Osaka, Japan). Con A was used at 5 μg/mL. Indomethacin was used at 5 μM. Phorbol 12-myristate 13-acetate (PMA) and ionomycin were from Sigma (St Louis, MO) and were used at concentrations of 50 ng/mL and 1 μg/mL, respectively. Antimouse CD3/CD28 beads (Dynal Biotech ASA, Oslo, Norway) were used at 10 μL per 10^6 cells. The transwell system with 1-μm pores for 12-well dishes was from BD Falcon (Franklin Lakes, NJ). Monoclonal antibodies for CD4, CD8, CD11b, CD25, CD29, CD44, CD45, CD69, Sca-1, B220, Gr-1, and interferon-γ (IFN-γ) were from BD Pharmingen (San Diego, CA). An inhibitor of IDO, 1-methyl-DL-tryptophan (1-MT), was purchased from Sigma. An antibody for TGF-β was purchased from Peprotech (Rocky Hill, NJ). Lipopolysaccharide was from Sigma.

MSCs

MSCs were obtained from wild-type or iNOS$^{-/-}$ C57BL/6 mice. Bone marrow cells were harvested from femurs and tibias by a standard flushing method[1] and then cultivated in a plastic dish in Iscove modified Dulbecco medium (Invitrogen, Carlsbad, CA) supplemented with 10% fetal calf serum (Sigma), 2 mM L-glutamine, 0.1 mg/mL streptomycin, and 100 U/mL penicillin G (Invitrogen) or in MF medium (Toyobo, Tokyo, Japan).

All primary MSCs were characterized at least once by flow cytometry and an in vitro differentiation assay. All MSCs were positive for CD29, CD44, and Sca-1, negative for CD11b, Gr-1, and CD45, and able to

Submitted February 13, 2006; accepted August 3, 2006. Prepublished online as *Blood* First Edition Paper, September 19, 2006; DOI 10.1182/blood-2006-02-002246.

The publication costs of this article were defrayed in part by page charge payment. Therefore, and solely to indicate this fact, this article is hereby marked "advertisement" in accordance with 18 USC section 1734.

differentiate into adipocytes and osteoblasts (Figure S1, available at the *Blood* website; see the Supplemental Figures link at the top of the online article). We used at least 2 independently isolated batches of MSCs. These cells can be propagated for a long time and retain their surface phenotype and capacity to differentiate for at least 4 months.

Flow cytometric analysis

Cells were incubated with Fc block (BD Pharmingen) to inhibit nonspecific binding of antibodies to Fc receptors. Next, cells were stained in FACS buffer (phosphate-buffered saline [PBS] supplemented with 10% fetal bovine serum) with antibodies for 30 minutes on ice, washed with FACS buffer, and analyzed on a BD LSR flow cytometer (Becton Dickinson, Franklin Lakes, CA). Collected data were analyzed with CELLQUEST software (Becton Dickinson).

Enzyme-linked immunosorbent assay (ELISA)

ELISA kits for mouse IFN-γ and mouse interleukin-2 (IL-2; BD Pharmingen) were used according to the manufacturer's instructions.

Selection of CD4+, CD8+, and CD19+ cells

$CD4^+$, $CD8^+$, and $CD19^+$ cells were selected using mouse CD4, CD8, and CD19 MACS beads and an autoMACS system (Miltenyi Biotech, Auburn, CA). The purity of the cells as determined by flow cytometry with antibodies against CD4, CD8, and B220 was more than 80%.

Thymidine incorporation

Splenocytes were grown in 96-well plates containing RPMI 1640 (Invitrogen) supplemented with 10% fetal calf serum (Sigma), 2 mM L-glutamine (Invitrogen), 50 μM 2-mercaptoethanol (Sigma), 0.1 mg/mL streptomycin, and 100 U/mL penicillin G (Invitrogen). During the cultivation, the cells were pulsed for the last 8 hours of culture with 1 mCi (3.7×10^7 Bq) of [^{3}H]-thymidine (Amersham Biosciences, Piscataway, NJ). After 48 hours of growth, cells were harvested with a Packard FilterMate harvester (Perkin Elmer Life Sciences, Boston, MA), transferred to a UniFilter plate (Perkin Elmer Life Sciences), and analyzed using a TopCount microplate scintillation counter (Perkin Elmer Life Sciences). In the coculture system, MSCs were γ-irradiated (30 Gy) prior to cultivation to prevent thymidine incorporation. When using the transwell system (BD Falcon), one tenth of the cells were harvested and counted because the system includes 12-well culture dishes, which contain 10-fold more cells than the wells of a 96-well plate.

Western blot analysis

Polyclonal antibodies to phosphorylated Stat5 (Cell Signaling Technology, Danvers, MA), Stat5 (Santa Cruz Biotechnology, Santa Cruz, CA), cyclin D2 (Cell Signaling Technology), and Kip1 (Cell Signaling Technology) were used for Western blotting. Cells were lysed on ice for 15 minutes with a buffer consisting of 50 mM Tris (pH 7.5), 150 mM NaCl, 0.5% NP40, Complete proteinase inhibitor cocktail (Roche Diagnostics, Mannheim, Germany), and 1 mM Na_3VO_4. Lysates were centrifuged at 13 000*g* for 15 minutes, and supernatants were subjected to sodium dodecyl sulfate–polyacrylamide gel electrophoresis (SDS-PAGE). Proteins were transferred from the gel to a PVDF membrane (Invitrogen), and Western blotting was performed using enhanced chemiluminescence reagents (Pierce, Rockford, IL) to visualize the immunoreactive proteins.

Assay for NO production

NO is quickly converted to NO_2 and NO_3 in culture medium. Because of the presence of NO_3 in RPMI medium, we measured NO_2 production using a Griess reagent kit (Wako).

Detection of iNOS expression

Total RNA was prepared using an RNeasy kit (Qiagen, Valencia, CA) and 1 μg was reverse-transcribed using a First Strand Synthesis Kit (Invitrogen), and one tenth of the product was subjected to PCR using the following primers: for iNOS, 5′-GAGATTGGAGTTCGAGACTTC-3′ and 5′-TGGCTAGTGCTTCAGACTTC-3′; and for β-actin, 5′-CCATCATGAAGTGTGACGTTG-3′ and 5′-GTCCGCCTAGAAGCACTTGCG-3′.

Western blotting was performed using a polyclonal antibody for iNOS (BD Transduction Laboratories, Lexington, KY) or a monoclonal antibody for β-actin (Sigma) to confirm equal loading. Immunofluorescence was carried out using the polyclonal iNOS antibody (BD Transduction Laboratories) followed by Alexa Fluor 488 goat anti–rabbit IgG (Molecular Probes, Eugene, OR). To distinguish splenocytes from MSCs, cells were simultaneously stained with phycoerythrin-conjugated anti-CD45 monoclonal antibody (BD Pharmingen). Cells were fixed with ProLong Gold antifade reagent (Molecular Probes) and were visualized by confocal microscopy (Nikon, Tokyo, Japan), and images were analyzed with the accompanying confocal image analysis software (Bio-Rad, Hercules, CA).

Intracellular staining

Intracellular staining was performed using a BD Cytofix/Cytoperm kit (BD Pharmingen) according to the manufacturer's instructions.

Mice

Wild-type mice (C57BL/6) were purchased from Clea Japan (Tokyo). The $iNOS^{-/-}$ mice (C57BL/6 background) were purchased from Jackson Laboratory (Bar Harbor, ME).

Cell lines

RAW264.7 mouse macrophage cells were a generous gift from Dr Matsuura (Jichi Medical University, Tochigi, Japan). HeLa human cervical carcinoma cells were used as negative control for iNOS expression.

Statistical analysis

We used the Student *t* test for statistical analysis. Differences were considered statistically significant at *P* values less than .05.

Results

Characteristics of T-cell suppression by MSCs

Although many reports[9-17,27] have shown that MSCs suppress T-cell proliferation, the molecular mechanisms and the signaling molecules inhibited by MSCs have not been defined. We therefore investigated the status of activated T cells in the presence of MSCs. The expression of activation markers and the production of IL-2 and IFN-γ were evaluated by flow cytometry, ELISA, and intracellular staining. The expression of the activation markers CD25 and CD69 on CD4 or CD8 T cells was not changed by the presence of MSCs (Figure 1A). In addition, MSCs suppressed the production of IFN-γ but not IL-2 (Figure 1B, upper panel). Also, IFN-γ production was diminished after 24 hours in the presence of MSCs (Figure 1B, lower panel). These findings are in agreement with previous results,[27] but they do not explain the strong suppression of T-cell proliferation by MSCs; for example, thymidine incorporation by T cells is reduced more than 10-fold in the presence of MSCs (data not shown).

We next induced T-cell proliferation using a combination of PMA and ionomycin, which act downstream of the T-cell–receptor complex by activating protein kinase C and inducing Ca^{2+} influx, respectively. This proliferation was suppressed by MSCs (Figure 1C), suggesting that the T-cell receptor complex is not a target for the suppression and that MSCs influence signals downstream of protein kinase C and Ca^{2+} influx. As demonstrated in Figure 1C, the proliferation of both purified CD4 and CD8 T cells as well as unfractionated splenocytes was suppressed by MSCs.

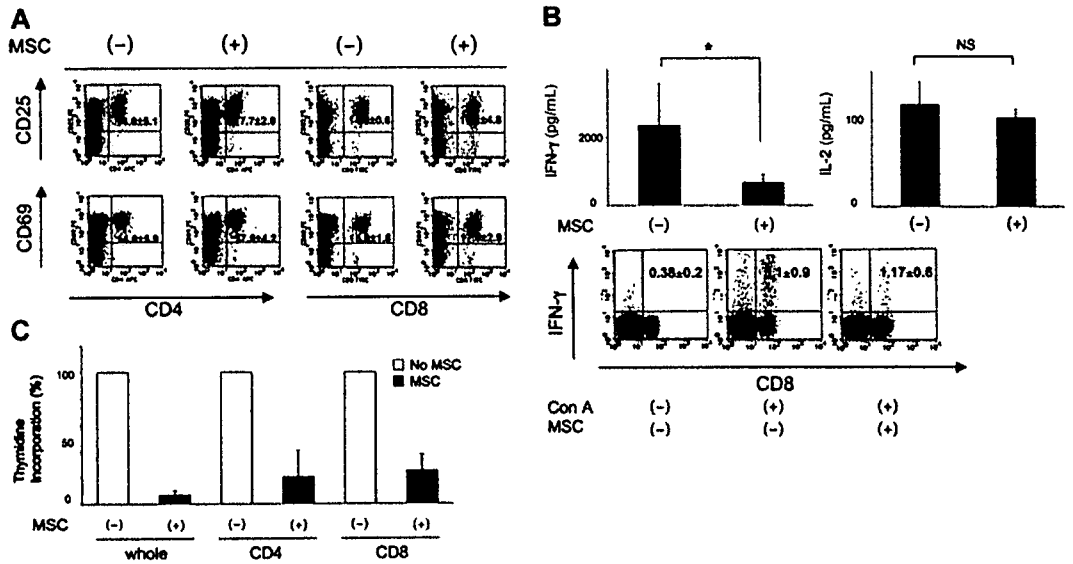

Figure 1. Status of activated T cells in the presence of MSCs. (A) Expression of the T-cell activation markers CD25 and CD69 on CD4 or CD8 cells 24 hours after stimulation of splenocytes (1×10^6 cells) in a 12-well dish with anti-CD3/CD28 beads (10 μL) in the presence or absence of 1×10^5 MSCs. The numbers in the top right quadrants indicate the percentage ± the standard deviation (SD). (B) Top panel, cytokine production in the same condition as in panel A. Concentrations of IL-2 and IFN-γ were determined at 48 hours by ELISA. The values are the means ± SD from 3 independent experiments. Bottom panel, intracellular staining of IFN-γ at 24 hours. GolgiStop (monensin) was used for the last 8 hours. The values are the mean percentages of CD8/IFN-γ–positive cells ± SD from 3 independent experiments. (C) MSCs suppress the induction of $CD4^+$ and $CD8^+$ T-cell proliferation by PMA and ionomycin. Splenocytes (1×10^5), $CD4^+$ cells (1×10^5), or $CD8^+$ cells (1×10^5) were stimulated in the presence or absence of irradiated MSCs (1×10^4) in the wells of a 96-well plate. The incorporation of [^{3}H]-thymidine is shown relative to that in the absence of MSCs. The values are the means ± SD from 3 independent experiments. *$P < .05$. NS indicates $P > .05$.

Stat5 phosphorylation is inhibited by MSCs

Although T cells from Stat5ab$^{-/-}$ mice do not proliferate upon stimulation with anti-CD3, they up-regulate CD25.[28] Because this phenotype is similar to the status of activated T cells in the presence of MSCs (Figure 1A), we hypothesized that they suppress Stat5 phosphorylation. Indeed, as shown in Figure 2, Stat5 phosphorylation was diminished in activated T cells in the presence of MSCs despite equivalent IL-2 production (Figure 1B). The reported changes in cell-cycle–related proteins, including the down-regulation of cyclin D2 and up-regulation of p27 Kip1 in the presence of MSCs,[27] were observed less consistently; in most cases, we found that MSCs up-regulated cyclin D2 and down-regulated p27 Kip1 in activated splenocytes compared with freshly isolated splenocytes (data not shown).

Dose dependency and time course of NO production

Macrophages have been reported to suppress T-cell proliferation[19-23] due to the production of NO and its inhibition of Stat5 phosphorylation.[18,19] This prompted us to examine the production of NO in our mouse MSC system. We found that MSCs caused a significant and dose-dependent production of NO (Figure 3A). NO could be first detected approximately 12 hours after the activation of T cells in the presence of MSCs. In the transwell system, in which the T cells were separated from the MSCs by a 1-μm-pore membrane, NO production was initially detected approximately 24 hours after the activation of T cells (Figure 3B).

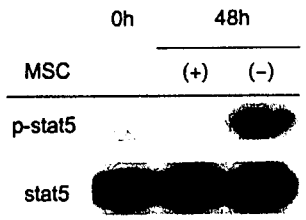

Figure 2. Inhibition of Stat5 phosphorylation in the presence of MSCs. Western blot analysis of Stat5 phosphorylation. Splenocytes (2×10^6) were activated with anti-CD3/CD28 beads in the presence or absence of 1×10^5 MSCs. After 48 hours, splenocytes were collected, lysed, and analyzed by Western blotting. Each lane contains 20 μg protein. Western blotting with anti-Stat5 is shown as a loading control. Shown are representative results from more than 5 experiments.

T-cell suppression and NO

Significant amounts of NO were not produced by MSCs cocultured with T cells in the absence of Con A or by Con A–treated MSCs or T cells (Figure 4A). In the presence of a direct interaction between T cells and MSCs, there was a high level of NO production accompanied by a strong suppression of T-cell proliferation (Figure 4A-B). In contrast, both NO production and T-cell suppression were reduced in a transwell system (Figure 4A-B). We further examined whether such a difference is observed using the RAW264.7 macrophage cell line, a well-characterized producer of NO. As with MSCs, T-cell suppression and NO production were inhibited in the transwell system using the RAW264.7 cells (Figure 4B, right side, and data not shown), suggesting that the difference reflects common aspects of T-cell suppression by NO.

T cells but not B cells induce NO

We next asked which cell type causes the NO production. We found that purified $CD4^+$ and $CD8^+$ T cells induce similar degrees of T-cell suppression as unfractionated splenocytes (Figure 1C). Therefore, it is not surprising that they also produce NO in the presence of MSCs (Figure 4C). Although MSCs suppress B-cell proliferation (~50%; data not shown), purified $CD19^+$ B cells did not appear to induce NO production in the presence of MSCs, suggesting that the mechanisms of B-cell and T-cell suppression are different.

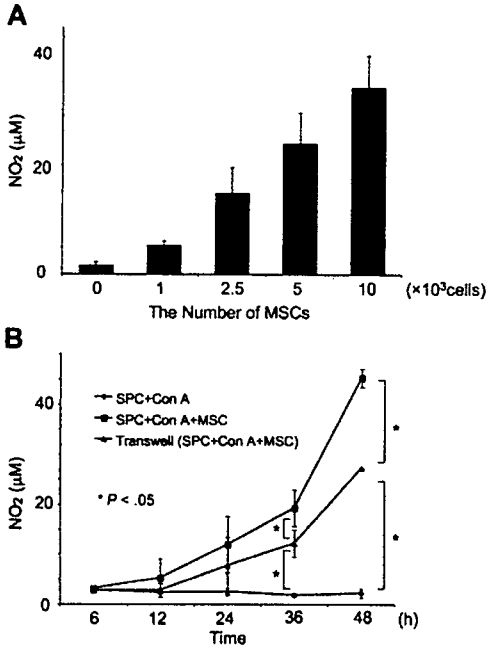

Figure 3. NO production in the presence of MSCs. (A) Dose-dependent effect of MSCs on NO production. Splenocytes (1×10^6) were activated with Con A (5 μg/mL) in the presence of the indicated number of MSCs for 48 hours in a 12-well dish. The concentrations of NO were determined by Griess assay. (B) Time course of NO production. MSCs (1×10^5/well) were treated as in panel A for the indicated amount of time. "Transwell" indicates experiments performed in 12-well dishes in which the T cells were separated from MSCs by a 1-μm-pore membrane. Values represent the means ± SD from 3 independent experiments. $^*P < .05$.

MSC–T-cell interaction and NO production

There are 2 possible explanations for the difference in NO production in the presence and absence of the transwell system. First, it is possible that there is a difference in the time course of NO production in the 2 systems. In the transwell system, a significant level of NO was typically detected after 24 hours, whereas NO production was detected after 12 to 18 hours in the presence of a direct interaction. Thus, the amount of NO produced in the transwell system was always lower than that in the presence of a direct interaction (Figure 3B). These findings suggest that a direct interaction is critical for the early and efficient production of NO as well as for the strong suppression of T-cell proliferation. A second possible explanation for the different results obtained in the transwell and direct interaction systems is that, because NO is highly unstable, in the transwell system it can lose its activity before it influences T cells.

MSCs are a producer of NO

If this second explanation is correct, MSCs should be the main producer of NO. Therefore, we examined whether MSCs can produce NO. It is known that there are 3 NO synthases (iNOS, endothelial NOS, and neuronal NOS), and only one of these, iNOS, can be induced by cell stimulation.[29] Therefore, we suspected that iNOS is induced in either T cells or MSCs. Reverse transcriptase–polymerase chain reaction (RT-PCR) (Figure 5A), Western blot analysis (Figure 5B), and immunofluorescence (Figure 5C) detected the induction of iNOS in MSCs cocultured with activated splenocytes but not in MSCs alone, splenocytes alone, or HeLa cells. The immunofluorescence studies showed that iNOS was exclusively expressed by large adherent $CD45^-$ cells, which correspond to MSCs (Figure 5C). In addition, iNOS appeared to be expressed throughout the cytoplasm as previously found in Kupffer cells and hepatocytes (Figure 5C).[30]

Specific inhibitor of NOS restores T-cell proliferation and Stat5 phosphorylation

Next, we investigated the effects of L-NAME, a specific inhibitor of NOS. As expected, L-NAME dose-dependently inhibited the production of NO by MSCs in the presence of activated T cells (Figure S2). Importantly, L-NAME restored T-cell proliferation (Figure 6A, left panel). The effect of L-NAME was dose dependent and more efficient when lower numbers of MSCs were used (Figure 6A, right panel). Using 2.5×10^3 MSCs, 1 mM L-NAME resulted in up to an approximately 80% recovery compared with the positive control (Figure 6A, left panel), suggesting that NO is one of the most important factors for T-cell suppression under the stringent conditions of our assays. On the other hand, even under these conditions, 100% recovery was not achieved, implying that other factors also contribute to the suppression of T-cell proliferation by MSCs.

L-NAME restored not only T-cell proliferation but also Stat5 phosphorylation (Figure 6B), indicating that NO inhibits Stat5 phosphorylation. Because Stat5 is required for T-cell division,[28] we suspect that NO first inhibits Stat5 phosphorylation, which then results in arrest of the cell cycle.

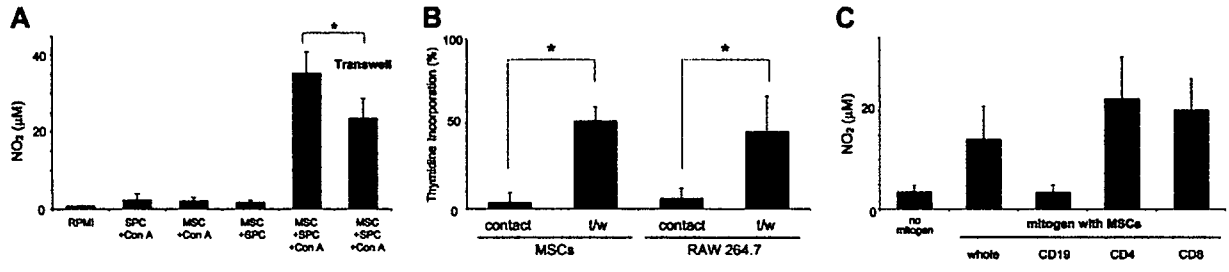

Figure 4. Relationship between NO production and T-cell suppression. (A) Production of NO. Splenocytes (1×10^6) were incubated with or without Con A in the presence or absence of MSCs for 48 hours. "Transwell" indicates experiments performed in 12-well dishes in which the T cells were separated from MSCs by a 1-μm-pore membrane. The values are the means ± SD from 3 independent experiments. $^*P < .05$. (B) T-cell proliferation in the presence or absence of the transwell system. Splenocytes (1×10^6) were activated with Con A in the presence or absence of 1×10^5 MSCs or RAW264.7 cells for 48 hours with or without the transwell. The incorporation of $[^3H]$-thymidine is shown relative to that in the absence of MSCs. The values are the means ± SD from 3 independent experiments. $^*P < .05$. (C) T cells but not B cells induce NO production. Purified CD4 or CD8 T cells (1×10^5; ~80% purity) induce NO in the presence of MSCs (1×10^4), whereas purified CD19 B cells (1×10^5; ~95% purity) do not induce significant NO production. The mitogen for T cells was Con A, and for B cells, it was lipopolysaccharide (1 μg/mL). The values are the means ± SD from 3 independent experiments. $^*P < .05$.

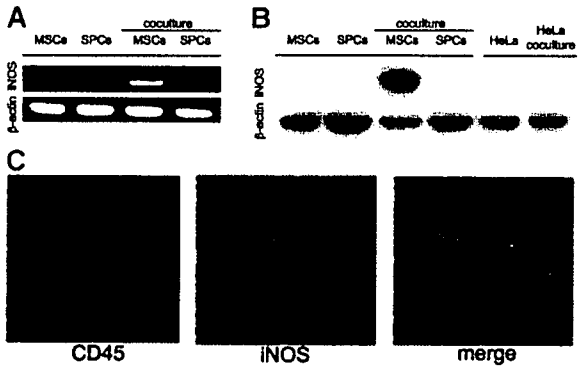

Figure 5. Induction of iNOS in MSCs. Total RNA and cell lysates were collected from MSCs alone, splenocytes alone, MSCs cocultured with activated T cells, or activated splenocytes cocultured with MSCs. MSCs were harvested just after washing out activated T cells with PBS. (A) RT-PCR analysis of iNOS mRNA. β-actin is shown as a control. (B) Western blot analysis of iNOS protein. Each lane contains 20 μg protein. β-actin is shown as a loading control. HeLa cells were used as negative control because the antibody also reacts with human iNOS protein. (C) Immunofluorescence of iNOS protein. Left panel, confocal immunofluorescent image of CD45 protein. Middle panel, confocal immunofluorescent image of iNOS protein. Right panel, merged confocal immunofluorescent images of CD45 protein and iNOS protein. Splenocytes (1×10^6) were activated with Con A in the presence of 1×10^5 MSCs for 48 hours. Images were visualized using a Nikon Eclipse TE300 microscope (Nikon, Tokyo, Japan) equipped with a 100×/1.40 numerical aperture oil objective lens, Nikon CFI Plan APO (Nikon). Images were acquired using Lasersharp software version 2.1 (Bio-Rad).

Other candidates as mediators of suppression by MSCs

Because TGF-β, IDO, and PGE_2 were reported as mediators of T-cell suppression by MSCs,[13-15] we further compared the effects of L-NAME with inhibitors of each mediator. Indomethacin (inhibitor of PGE_2 production) but not 1-MT (inhibitor of IDO) or an anti–TGF-β–neutralizing antibody restored T-cell proliferation as effectively as L-NAME (Figure 7A); however, the effects of L-NAME and indomethacin were not additive, suggesting that the NO and PGE_2 share signaling pathways leading to T-cell suppression (Figure 7A).

MSCs from iNOS$^{-/-}$ mice have reduced activity in T-cell suppression

Finally, we used MSCs from iNOS$^{-/-}$ mice to confirm that NO is produced by MSCs and that NO suppresses T-cell proliferation. MSCs from iNOS$^{-/-}$ mice were less effective than MSCs from wild-type mice at suppressing T-cell proliferation, suggesting that NO produced by MSCs is a major mediator of this effect (Figure 7B, left panel). We also confirmed that MSCs from iNOS$^{-/-}$ mice do not produce NO even in the presence of activated T cells (Figure 7B, right panel).

Discussion

Here, we demonstrate for the first time that the production of NO is involved in the suppression of T cells by MSCs. We also showed that NO inhibits Stat5 phosphorylation. Although NO was already known to suppress T-cell proliferation, NO has not been previously reported to mediate T-cell suppression by MSCs.[29] Our hypothesis that NO is produced by MSCs and that it suppresses T-cell proliferation in part through Stat5 inhibition was supported by the following facts: (1) NO was readily detected in the medium in the presence of MSCs; (2) L-NAME restored T-cell proliferation as well as Stat5 phosphorylation; and (3) MSCs from iNOS$^{-/-}$ mice had markedly reduced abilities to suppress T-cell proliferation. This hypothesis was further confirmed by the finding that iNOS was detected only in MSCs.

Compared with experiments in which cells were in direct contact, experiments performed in transwells showed a lag in NO production, suggesting that T-cell–MSC contact is critical for the early and efficient production of NO and, thus, T-cell suppression. Whether a soluble factor is a main mediator of T-cell suppression by MSCs has been controversial because results from transwell systems have been inconsistent.[12,14,16-17] Our finding that the transwell reduces but does not abolish T-cell suppression (Figure 4B) may help explain these conflicting reports. Although we could not define the mechanism by which NO production is suppressed in the transwell system, the amount of NO production appears to correspond with the extent of T-cell suppression.

Under stringent conditions, in which a lower number of MSCs was used, the restoration of T-cell proliferation by L-NAME reached up to approximately 80%, suggesting that NO is one of the major mediators; however, 100% restoration was never attained, suggesting that other factor(s) contribute to the suppression. Because TGF-β, IDO, and PGE_2 have been considered as possible mediators of T-cell suppression by MSCs,[13-15] we examined the effect of specific inhibitors of each. We found that indomethacin (inhibitor of PGE_2 production) restores T-cell proliferation as previously reported[15] but that neither 1-MT (inhibitor of IDO) nor the TGF-β antibody had an effect. Also, the effects of indomethacin

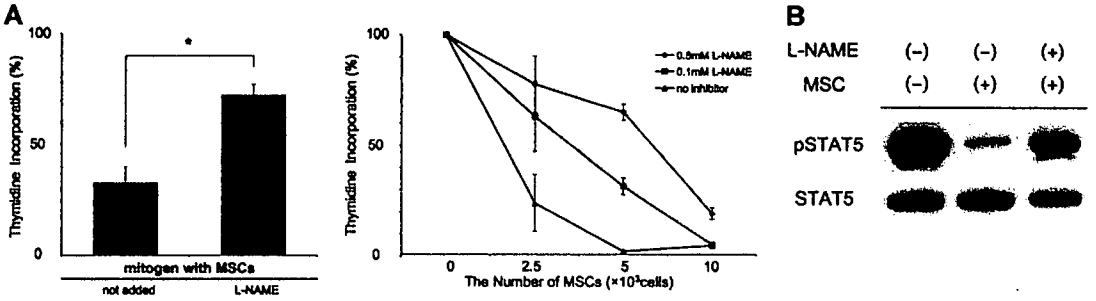

Figure 6. A specific inhibitor of NOS restores T-cell proliferation and Stat5 phosphorylation. (A) Effect of L-NAME on thymidine incorporation. Top panel, splenocytes (1×10^5) were activated with Con A in the presence or absence of 2.5×10^3 irradiated MSCs and in the presence or absence of 1 mM L-NAME. The incorporation of [^{3}H]-thymidine is shown relative to that in the absence of MSCs. The values are the means ± SD from 3 independent experiments. *$P < .05$. Bottom panel, dose-dependent restoration of T-cell proliferation by L-NAME. Splenocytes (1×10^5) were activated with Con A in the presence of the indicated number of irradiated MSCs for 48 hours. The concentrations of L-NAME are shown. Shown is a typical result of 3 independent experiments. (B) L-NAME restores Stat5 phosphorylation. Splenocytes (2×10^6) were activated with anti-CD3/CD28 beads in the presence or absence of 0.5×10^5 to 1×10^5 MSCs for 48 hours and in the presence or absence of 1 mM L-NAME. Western blotting for phosphorylated and total Stat5 was performed as described in Figure 2. Shown is a representative result from 5 independent experiments.

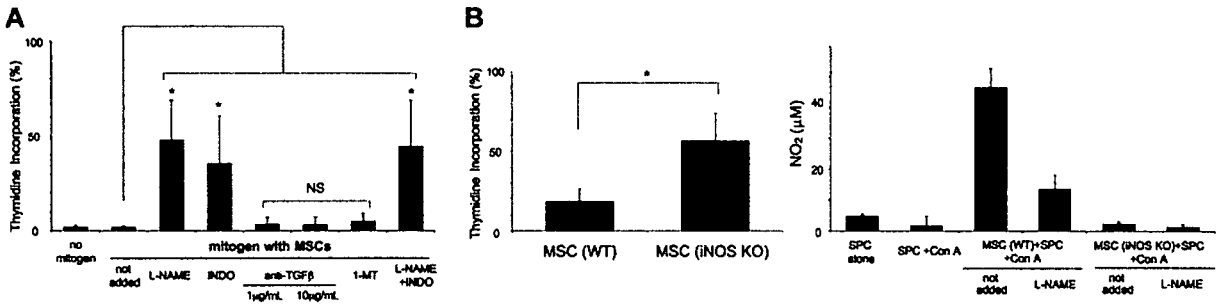

Figure 7. Effect of inhibitors and T-cell suppression by MSCs from iNOS$^{-/-}$ mice. (A) L-NAME and indomethacin (INDO) restored T-cell proliferation, but TGF-β antibody and 1-MT had no effect. Splenocytes (1×10^5) were activated with Con A in the presence or absence of irradiated MSCs (2.5×10^3), 1 mM L-NAME, 5 μM indomethacin,[14] 1 μg/mL or 10 μg/mL TGF-β antibody, and 1 mM 1-MT for 48 hours. The incorporation of [^{3}H]-thymidine is shown relative to that in the absence of MSCs. Shown is the mean ± SD of 3 independent experiments. *$P < .05$. NS indicates $P > .05$. (B) MSCs from iNOS$^{-/-}$ mice have a reduced ability to inhibit T-cell proliferation. Splenocytes (1×10^5) were activated with Con A in the presence or absence of MSCs (2.5×10^3) from either wild-type or iNOS$^{-/-}$ mice. Left panel, incorporation of [^{3}H]-thymidine relative to that in the absence of MSCs. Right panel, production of NO. The values are the means ± SD from 3 independent experiments. *$P < .05$.

were not additive with those of L-NAME. These results, combined with previous reports,[31,32] suggest that NO acts upstream of PGE_2. Furthermore, our results imply that NO may be the central mediator of T-cell proliferation.

Under our standard conditions (1:10 ratio of MSCs to splenocytes), 1 mM L-NAME restored T-cell proliferation to approximately 25%. Similarly, 5 μM indomethacin also produced an approximately 25% recovery (data not shown). These results suggest that the restoration by L-NAME or indomethacin is not specific to the more stringent conditions (1:40 ratio of MSCs to splenocytes).

Although most of the results from our mouse MSC system are consistent with previous reports,[12,15,27] we did not find a clear correlation between T-cell suppression and the up-regulation of Kip1 or the down-regulation of cyclin D2. Instead, our results suggest that the inhibition of Stat5 phosphorylation is more important for T-cell suppression, at least under the conditions of our experiments. In the conditions studied here, after coculture with MSCs, T cells could respond to a second mitogenic stimulation (data not shown), whereas they could not respond to a second stimulation in a previous report,[27] suggesting that the status of T cells in our experiments is different than that in the previous report.

Our results provide new insight into how MSCs modulate immune function. Although it is known that the NO-Stat5 pathway is important for T-cell suppression by macrophages, this is the first report demonstrating that the NO-Stat5 pathway is also critical for T-cell suppression by MSCs. The physiologic role of NO produced by MSCs is unknown, and we are currently investigating the possibility that MSCs in bone marrow protect hematopoietic stem cells from T-cell–mediated destruction by inhibiting T-cell proliferation.

Acknowledgments

We would like to thank Dr Hitoshi Endo (Jichi Medical University) for technical assistance with immunofluorescence microscopy, Dr David Munn (MCG Immunotherapy Center, Medical College of Georgia, Augusta) for technical advice with dissolving 1-MT, and Dr Motohiro Matsuura (Jichi Medical University) for providing the RAW264.7 macrophage cell line.

This work was supported in part by grants from the Ministry of Health, Welfare, and Labor of Japan and Grants-in-Aid for Scientific Research from the Ministry of Education, Science, Sports, and Technology of Japan.

Authorship

Contribution: K.S. performed the research and analyzed data; K. Ozaki designed the research and wrote the paper; K.H. performed Western blotting; I.O. carried out experiments regarding PMA plus ionomycin; T.N. provided technical advice; A.M. and K.M. provided some reagents and analyzed data; and K. Ozawa organized the research project.

Conflict-of-interest disclosure: The authors declare no competing financial interests.

Correspondence: Katsutoshi Ozaki, Division of Hematology, Jichi Medical University; 3311-1 Yakushiji, Shimotsuke-shi, Tochigi 329-0498, Japan; e-mail: ozakikat@jichi.ac.jp; and Keiya Ozawa, Division of Hematology, Jichi Medical University; 3311-1 Yakushiji, Shimotsuke-shi, Tochigi 329-0498, Japan; e-mail: kozawa @ms2.jichi.ac.jp.

References

1. Meirelles Lda S, Nardi NB. Murine marrow-derived mesenchymal stem cell: isolation, in vitro expansion, and characterization. Br J Haematol. 2003;123:702-711.
2. Pittenger MF, Mackay AM, Beck SC, et al. Multilineage potential of adult human mesenchymal stem cells. Science. 1999;284:143-147.
3. Kawada H, Fujita J, Kinjo K, et al. Nonhematopoietic mesenchymal stem cells can be mobilized and differentiate into cardiomyocytes after myocardial infarction. Blood. 2004;104:3581-3587.
4. Koc ON, Gerson SL, Cooper BW, et al. Rapid hematopoietic recovery after coinfusion of autologous-blood stem cells and culture-expanded marrow mesenchymal stem cells in advanced breast cancer patients receiving high-dose chemotherapy. J Clin Oncol. 2000;18:307-316.
5. Noort WA, Kruisselbrink AB, in't Anker PS, et al. Mesenchymal stem cells promote engraftment of human umbilical cord blood-derived CD34(+) cells in NOD/SCID mice. Exp Hematol. 2002;30:870-878.
6. in't Anker PS, Noort WA, Kruisselbrink AB, et al. Nonexpanded primary lung and bone marrow-derived mesenchymal cells promote the engraftment of umbilical cord blood-derived CD34(+) cells in NOD/SCID mice. Exp Hematol. 2003;31:881-889.
7. Koc ON, Peters C, Aubourg P, et al. Bone marrow-derived mesenchymal stem cells remain host-derived despite successful hematopoietic engraftment after allogeneic transplantation in patients with lysosomal and peroxisomal storage diseases. Exp Hematol. 1999;27:1675-1681.
8. Bensidhoum M, Chapel A, Francois S, et al. Homing of in vitro expanded Stro-1$^-$ or Stro-1$^+$ human mesenchymal stem cells into the NOD/SCID mouse and their role in supporting human CD34 cell engraftment. Blood. 2004;103:3313-3319.
9. Maitra B, Szekely E, Gjini K, et al. Human mesenchymal stem cells support unrelated donor hematopoietic stem cells and suppress T-cell activation. Bone Marrow Transplant. 2004;33:597-604.
10. Beyth S, Borovsky Z, Mevorach D, et al. Human mesenchymal stem cells alter antigen-presenting

cell maturation and induce T-cell unresponsiveness. Blood. 2005;105:2214-2219.

11. Groh ME, Maitra B, Szekely E, et al. Human mesenchymal stem cells require monocyte-mediated activation to suppress alloreactive T cells. Exp Hematol. 2005;33:928-934.
12. Krampera M, Glennie S, Dyson J, et al. Bone marrow mesenchymal stem cells inhibit the response of naive and memory antigen-specific T cells to their cognate peptide. Blood. 2003;101: 3722-3729.
13. Di Nicola M, Carlo-Stella C, Magni M, et al. Human bone marrow stromal cells suppress T-lymphocyte proliferation induced by cellular or nonspecific mitogenic stimuli. Blood. 2002;99: 3838-3843.
14. Meisel R, Zibert A, Laryea M, Gobel U, Daubener W, Dilloo D. Human bone marrow stromal cells inhibit allogeneic T-cell responses by indoleamine 2,3-dioxygenase-mediated tryptophan degradation. Blood. 2004;103:4619-4621.
15. Aggarwal S, Pittenger MF. Human mesenchymal stem cells modulate allogeneic immune cell responses. Blood. 2005;105:1815-1822.
16. Tse WT, Pendleton JD, Beyer WM, Egalka MC, Guinan EC. Suppression of allogeneic T-cell proliferation by human marrow stromal cells: implications in transplantation. Transplantation. 2003;75: 389-397.
17. Djouad F, Plence P, Bony C, et. al. Immunosuppressive effect of mesenchymal stem cells favors tumor growth in allogeneic animals. Blood. 2003; 102:3837-3844.
18. Mazzoni A, Bronte V, Visintin A, et al. Myeloid suppressor lines inhibit T cell responses by an NO-dependent mechanism. J Immunol. 2002; 168:689-695.
19. Bingisser RM, Tilbrook PA, Holt PG, Kees UR. Macrophage-derived nitric oxide regulates T cell activation via reversible disruption of the Jak3/ STAT5 signaling pathway. J Immunol. 1998;160: 5729-5734.
20. Albina JE, Abate JA, Henry WL Jr. Nitric oxide production is required for murine resident peritoneal macrophages to suppress mitogen-stimulated T cell proliferation: role of IFN-gamma in the induction of the nitric oxide-synthesizing pathway. J Immunol. 1991;147: 144-148.
21. Young MR, Wright MA, Matthews JP, Malik I, Prechel M. Suppression of T cell proliferation by tumor-induced granulocyte-macrophage progenitor cells producing transforming growth factor-beta and nitric oxide. J Immunol. 1996;156:1916-1922.
22. Medot-Pirenne M, Heilman MJ, Saxena M, McDermott PE, Mills CD. Augmentation of an antitumor CTL response in vivo by inhibition of suppressor macrophage nitric oxide. J Immunol. 1999;163:5877-5882.
23. Lejeune P, Lagadec P, Onier N, Pinard D, Ohshima H, Jeannin JF. Nitric oxide involvement in tumor-induced immunosuppression. J Immunol. 1994;152:5077-5083.
24. Angulo I, de las Heras FG, Garcia-Bustos JF, Gargallo D, Munoz-Fernandez MA, Fresno M. Nitric oxide-producing CD11b(+)Ly-6G(Gr-1)(+)CD31(ER-MP12)(+) cells in the spleen of cyclophosphamide-treated mice: implications for T-cell responses in immunosuppressed mice. Blood. 2000;95:212-220.
25. Bobe P, Benihoud K, Grandjon D, Opolon P, Pritchard LL, Huchet R. Nitric oxide mediation of active immunosuppression associated with graft-versus-host reaction. Blood. 1999;94:1028-1037.
26. Mais A, Klein T, Ullrich V, Schudt C, Lauer G. Prostanoid pattern and iNOS expression during chondrogenic differentiation of human mesenchymal stem cells. J Cell Biochem. 2005;94:307-316.
27. Glennie S, Soeiro I, Dyson PJ, Lam EW, Dazzi F. Bone marrow mesenchymal stem cells induce division arrest anergy of activated T cells. Blood. 2005;105:2821-2827.
28. Moriggl R, Topham DJ, Teglund S, et al. Stat5 is required for IL-2-induced cell cycle progression of peripheral T cells. Immunity. 1999;10:249-259.
29. Bogdan C. Nitric oxide and the immune response. Nat Immunol. 2001;2:907-916.
30. Stolz DB, Zamora R, Vodovotz Y, et al. Peroxisomal localization of inducible nitric oxide synthase in hepatocytes. Hepatology. 2002;36:81-93.
31. Kim SF, Huri DA, Snyder SH. Inducible nitric oxide synthase binds, S-nitrosylates, and activates cyclooxygenase-2. Science. 2005;310:1966-1970.
32. Clancy R, Varenika B, Huang W, et al. Nitric oxide synthase/COX cross-talk: nitric oxide activates COX-1 but inhibits COX-2-derived prostaglandin production. J Immunol. 2000;165:1582-1587.

Protection Against Aminoglycoside-induced Ototoxicity by Regulated AAV Vector–mediated GDNF Gene Transfer Into the Cochlea

Yuhe Liu[1,2,3], Takashi Okada[1,4], Kuniko Shimazaki[5], Kianoush Sheykholeslami[6], Tatsuya Nomoto[1], Shin-Ichi Muramatsu[7], Hiroaki Mizukami[1], Akihiro Kume[1], Shuifang Xiao[3], Keiichi Ichimura[2] and Keiya Ozawa[1]

[1]Division of Genetic Therapeutics, Jichi Medical University, Tochigi, Japan; [2]Department of Otolaryngology, Jichi Medical University, Tochigi, Japan; [3]Department of Otolaryngology, Peking University First Hospital, Beijing, China; [4]Department of Molecular Therapy, National Institute of Neuroscience, National Center of Neurology and Psychiatry, Tokyo, Japan; [5]Department of Physiology, Jichi Medical University, Tochigi, Japan; [6]Department of Neurobiology, Northeastern Ohio Universities College of Medicine, Rootstown, Ohio, USA; [7]Division of Neurology, Department of Medicine, Jichi Medical University, Tochigi, Japan

Since standard aminoglycoside treatment progressively causes hearing disturbance with hair cell degeneration, systemic use of the drugs is limited. Adeno-associated virus (AAV)-based vectors have been of great interest because they mediate stable transgene expression in a variety of postmitotic cells with minimal toxicity. In this study, we investigated the effects of regulated AAV1-mediated glial cell line–derived neurotrophic factor (GDNF) expression in the cochlea on aminoglycoside-induced damage. AAV1-based vectors encoding GDNF or vectors encoding GDNF with an rtTA2s-S2 Tet-on regulation system were directly microinjected into the rat cochleae through the round window at 5×10^{10} genome copies/body. Seven days after the virus injection, a dose of 333 mg/kg of kanamycin was subcutaneously given twice daily for 12 consecutive days. GDNF expression in the cochlea was confirmed and successfully modulated by the Tet-on system. Monitoring of the auditory brain stem response revealed an improvement of cochlear function after GDNF transduction over the frequencies tested. Damaged spiral ganglion cells and hair cells were significantly reduced by GDNF expression. Our results suggest that AAV1-mediated expression of GDNF using a regulated expression system in the cochlea is a promising strategy to protect the cochlea from aminoglycoside-induced damage.

Received 12 May 2007; accepted 15 November 2007; published online 8 January 2008. doi:10.1038/sj.mt.6300379

INTRODUCTION

Aminoglycoside antibiotics are frequently used in empiric therapy for serious infections, such as septicemia, complicated intra-abdominal infections, complicated urinary tract infections, and nosocomial respiratory tract infections. However, it is well known that aminoglycosides are associated with severe side effects, such as ototoxicity and nephrotoxicity, which attack the cochlea or vestibule and destroys the auditory and vestibular hair cells that pass information to the auditory nerve.[1] In addition, aminoglycosides predominantly destroy the outer hair cells by ototoxicity. Although the exact mechanism of damage is not well established,[2] aminoglycoside-induced hair cell loss results in a permanent hearing deficit[3] that can progressively occur 6 months to a year after exposure to these drugs. Therefore, the development of a strategy to prevent aminoglycoside-associated ototoxicity before adverse events occur is a critical issue in clinical settings.

The expression of a transgene using viral vectors is a potential approach to introduce neurotrophic factors into the cochlea to prevent and treat aminoglycoside-induced hearing loss. However, most of the currently used vectors, such as adenovirus vectors or herpes simplex virus vectors, have an associated vector-related cytotoxicity.[4,5] Hence, adeno-associated virus (AAV) vectors may be good candidates for gene transfer into the cochlear cells because of their efficient transduction and their safety and potential in long-term expression.[6] We have previously demonstrated that an AAV1-based vector efficiently transduced the inner hair cells, the spiral ganglion cells, and many other types of cells.[7] Therefore, an AAV1-based vector should successfully introduce secretory proteins, such as glial cell line–derived neurotrophic factor (GDNF), into the cochlea to prevent aminoglycoside-induced ototoxicity.

GDNF, a member of the transforming growth factor β family, was initially identified as a survival factor for mid-brain dopaminergic neurons and for a wide range of neuronal populations in the central and peripheral nervous systems.[8–10] Although it is still unclear whether GDNF protects against ototoxicity, sustained infusion of recombinant GDNF protected the cochlear structure and function from noise- and drug-induced damage and stress,[11–18] although its half-life is very short. However, an overdose of GDNF was shown to enhance the sensitivity of the cochleae to insult and

Correspondence: *Takashi Okada, Department of Molecular Therapy, National Institute of Neuroscience, National Center of Neurology and Psychiatry, 4-1-1 Ogawa-Higashi, Kodaira, Tokyo 187-8551, Japan. E-mail: t-okada@ncnp.go.jp; Keiya Ozawa, Division of Genetic Therapeutics, Center for Molecular Medicine, Jichi Medical University, 3311-1 Yakushiji, Shimotsuke, Tochigi 329-0498, Japan. E-mail: kozawa@jichi.ac.jp*

to destroy cochlear function.[12] Furthermore, it has been reported that testicular tumors are formed in GDNF-overexpressing mice.[19] Therefore, an appropriate regulation system is required to realize the therapeutic benefits of GDNF expression.

Regulated transgene expression has been successfully achieved in various gene therapy experiments using the Tet system.[20–23] Notably, tetracycline derivatives, such as doxycycline (Dox), activate the Tet-on system at doses 100-fold lower than tetracycline. Furthermore, the reverse Tet-responsive transcriptional activator (rtTA) series were improved through the generation of variants called rtTA2s-S2, which showed lower leakiness and better inducibility in HeLa cells and mice.[24,25]

In this study, we describe *in vivo* therapeutic experiments utilizing AAV1 vector–mediated tetracycline-regulated expression of GDNF in cochleae. We demonstrate that AAV1 vector–mediated GDNF expression protects sensory cells in the inner ear from drug-induced degeneration.

RESULTS

Expression and distribution of transgene in the cochlea

AAV1-EGFP or AAV1-GDNF containing either the enhanced humanized green fluorescent protein (*EGFP*) gene or the *GDNF* gene under the control of the CAG (human cytomegalovirus (CMV) immediate-early enhancer and Chicken β-actin promoter) promoter, and the Woodchuck hepatitis virus posttranscriptional regulatory element (WPRE) (**Figure 1a**), was injected into the cochlea. The GDNF protein level in the perilymph was measured by enzyme-linked immunosorbent assay (**Figure 2a**). There was a significant increase in GDNF concentration in the cochlea transduced with AAV1-GDNF. The widespread distribution of the GDNF expression was observed in the cochlea, including the spiral ganglion and the inner hair cells (**Figure 2b**).

To examine the possible transduction of the contralateral ear with the virus diffusion, we analyzed the AAV vector–meditated transgene expression of the rodents with this transduction approach using the optical bioluminescence imaging. Luciferase expression was mainly detected at the injected side of the cochleae (5,370.3 photons/sec/cm²/sr, **Supplementary Figure S1**). Interestingly, the AAV vector also transduced the contralateral ear (876.8 photons/sec/cm²/sr), along with the brain (792.9 photons/sec/cm²/sr). Similar results were obtained with repeated experiments.

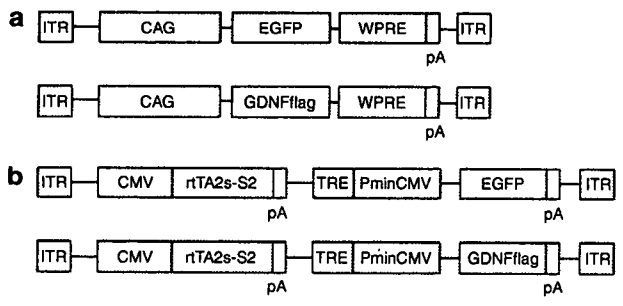

Figure 1 Schematic representation of the viral vectors used in this study. (**a**) An adeno-associated virus 1 (AAV1)-based vector was constructed using the CAG promoter to drive enhanced green fluorescent protein (EGFP) or mouse glial cell line–derived neurotrophic factor (GDNF) with a FLAG tag (GDNFflag). The Woodchuck hepatitis virus posttranscriptional regulatory element (WPRE) was inserted into the 3′ end of the transgene cassette. (**b**) The transactivator rtTA2s-S2 is under the control of the CMV promoter. The minimal CMV promoter (PminCMV) induces transgene expression (EGFP or GDNFflag) in combination with the Tetracycline-responsive element (TRE) and transactivator. CAG, human cytomegalovirus immediate-early enhancer and Chicken β-actin promoter; CMV, cytomegalovirus immediate-early promoter; pA, the simian virus 40 polyadenylation sequences; ITR, inverted terminal repeat from AAV2.

Preservation of the hair cells and spiral ganglion cells in the cochlea

Hair cell loss in the whole-mount cochleae of all the tested rat groups was analyzed by F-actin staining with rhodamine–phalloidin. **Figure 3a** shows a representative dissection through the second turn of the rat cochlea, in which a full complement of hair cells is revealed by F-actin phalloidin staining. In the vehicle-treated control group, outer hair cells in the base and middle turn were drastically lost after kanamycin treatment (**Figure 3b**). In the AAV1-GDNF/kanamycin-treated group, successful protection of the hair cells in the cochlea was observed (**Figure 3c**). In the contralateral cochlea, some of outer hair cells were also protected (**Figure 3d**). The spiral ganglion cell loss in the basal turn of the cochlea was assessed using 4′,6-diamino-2-phenylindole dihydrochloride staining (**Figure 4a** and **b**). Survival of the spiral ganglion cells in the AAV1-GDNF injected cochlea was significantly improved compared to that in the AAV1-EGFP injected cochlea (**Figure 4c**).

Protection of cochlear function by GDNF

Auditory brain stem response (ABR) recordings of the aminoglycoside-treated animals were performed to examine hearing

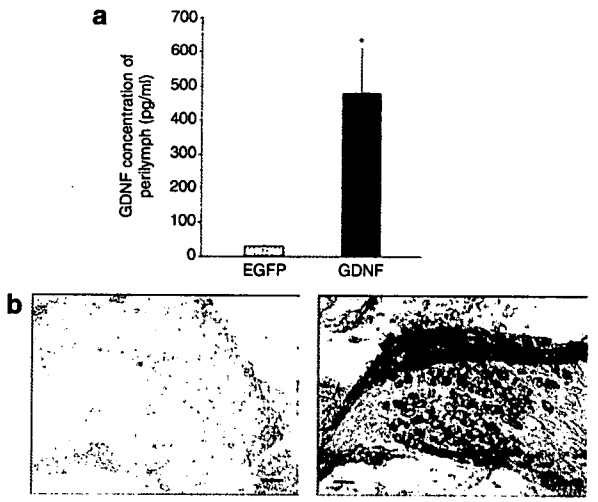

Figure 2 Expression and distribution of transgene in the cochlea. (**a**) Cochlear glial cell line–derived neurotrophic factor (GDNF) expression levels were measured by enzyme-linked immunosorbent assay in the transduced rats. GDNF expression level of the perilymph in the AAV1-GDNF/kanamycin group was significantly higher than that in the control group ($n = 5$, $P < 0.001$). (**b**) Immunohistochemistry was performed to analyze the expression of the GDNFflag in the rat cochlea. The AAV1-EGFP-transduced cochlea was used as a control (left). Cochlear sections were prepared after AAV1-GDNF injection and kanamycin administration. GDNflag expression was detected in the cochlea with an anti-FLAG antibody (right). Scale bar = 25 μm; ×400. AAV1, adeno-associated virus 1; EGFP, enhanced green fluorescent protein.

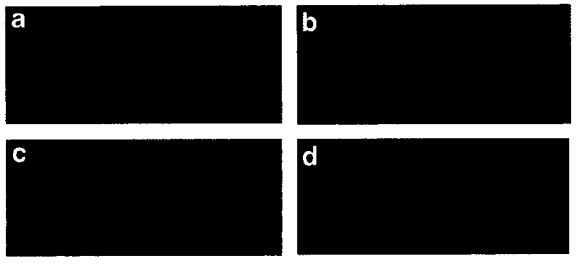

Figure 3 Preservation of the hair cells in the transduced cochlea. Hair cell loss in the cochlea of transduced rats was analyzed by F-actin staining. The dissected samples were dissected from the middle turn of the cochlea. The adeno-asssociated virus 1 (AAV1) vector was injected into the scala tympani of the cochlea prior to 12 days of kanamycin administration. (**a**) The normal cochlea. (**b**) The cochlea from the vehicle-treated ear; the many dark spaces represent the loss of outer hair cells. (**c**) The cochlea from the AAV1-GDNF-transduced ear. (**d**) The cochlea from the contralateral ear of AAV1-GDNF transduced rats. GDNF, glial cell line–derived neurotrophic factor.

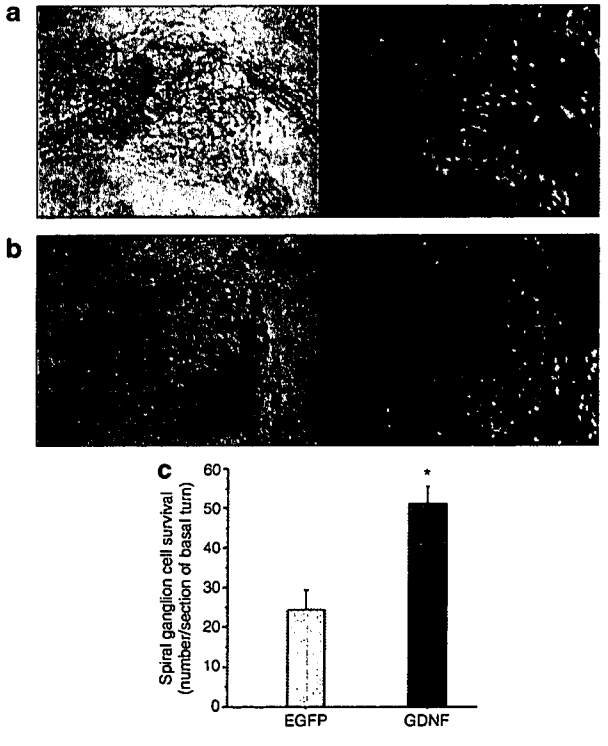

Figure 4 Survival of the spiral ganglion cells in the transduced cochlea. AAV1-GDNF-mediated rescue of the kanamycin-induced damage to the rat spiral ganglion neurons (SGNs): 4′,6-diamino-2-phenylindole dihydrochloride (DAPI) staining was performed on the sections obtained from the rat pretreated with either AAV1-EGFP or AAV1-GDNF, followed by kanamycin injections. (**a**, **b**) Representative photomicrographs of the cryosections showing the basal turn of the cochlear spiral (**a**, AAV1-EGFP; **b**, AAV1-GDNF). (**c**) The number of DAPI-positive large-nucleus cells that exhibited SGN morphology was counted. An asterisk denotes a statistically significant difference between the AAV1-GDNF and AAV1-EGFP-transduced rats (*t*-test, $P < 0.001$). AAV1, adeno-associated virus 1; EGFP, enhanced green fluorescent protein; glial cell line–derived neurotrophic factor.

impairment. At all frequencies tested, both GDNF-transduced and contralateral, untreated ears showed a significant improvement in the threshold shifts compared to the ears transduced with EGFP ($n = 5$, $P < 0.05$) (**Figure 5**). In the EGFP group, there was

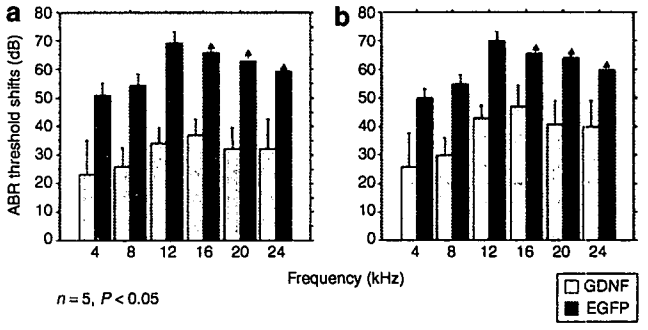

Figure 5 Protection of cochlear function by glial cell line–derived neurotrophic factor GDNF. Auditory brain stem response (ABR) threshold shifts (mean ± SD) of the (**a**) treated and (**b**) untreated ears at each tested frequency in the enhanced green fluorescent protein (EGFP) and GDNF transduced rats. The ABR threshold was measured twice in all the animals. The ears treated with AAV1-GDNF showed a significant improvement in the threshold shifts compared to the ears treated with AAV1-EGFP at all frequencies tested ($n = 5$, $P < 0.05$). Arrows indicate the average ABR thresholds that exceeded the output power of the ABR apparatus. AAV1, adeno-associated virus 1.

no significant difference in the ABR threshold shifts between the transduced and contralateral, untreated cochleae at all frequencies tested. Animals transduced with the AAV1-GDNF demonstrated lower ABR threshold shifts in the injected side compared to the contralateral side (at 12, 16, 20, 24 kHz; $P < 0.05$). These data indicate that both ears were protected even if the AAV1-GDNF was only injected into one ear.

Induced transgene expression

Two hundred and ninety three cells were transduced with the proviral plasmid harboring rtTA2s-S2 and the tetracycline-responsive element (TRE) to express the *EGFP* gene (**Figure 1b**). In the presence of Dox, a significant level of fluorescence was detected, suggesting that the rtTA2s-S2 system could switch on transcription following Dox treatment (**Figure 6a**). In contrast, reporter gene expression in the cultured cells was faint in the absence of Dox, indicating a low basal activity *in vitro*. Western blot analysis of GDNF showed that the transgene was induced in the presence of Dox, while no expression was detected in the absence of Dox (**Figure 6b**).

In vivo induction of GDNF expression and the dose–response to Dox

Enzyme-linked immunosorbent assay analysis of the GDNF expression level in muscle also showed low basal activity and induced expression after Dox treatment (**Figure 6c**). In the absence of Dox, the expression level of GDNF in the AAV2-S2-GDNF group was as low as that in the phosphate-buffered saline and AAV2-*LacZ* groups. On the other hand, significant increases in the GDNF level were observed in the muscle with increasing amounts of Dox, demonstrating that the rtTA2s-S2 system induces gene expression in a dose-dependent manner.

Inducible GDNF expression in the cochlea

Extensive inducible GDNF transgene expression was confirmed by immunohistochemistry using an anti-FLAG-antibody in the AAV1-S2-GDNF/kanamycin group in the presence of Dox (**Figure 7**).

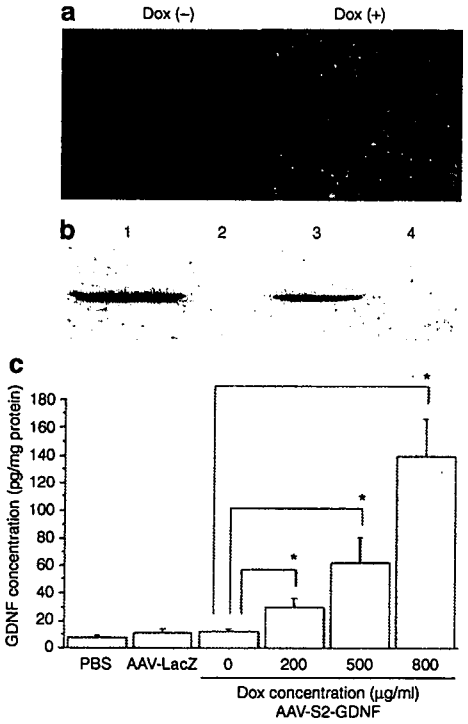

Figure 6 Induction of the transgene expression. (**a**) HEK293 cells were transfected with the proviral plasmid pAAV2-rtTA-S2-TRE-d2EGFP, and the expression of enhanced green fluorescent protein (EGFP) was induced by the doxycycline (Dox) (1 μg/ml). (**b**) Western blot analysis with an anti-FLAG antibody to detect the glial cell line–derived neurotrophic factor (GDNF) expression in the transduced 293 cells with the proviral plasmids. pAAV2-GDNF (lane 1), pAAV2-EGFP (lane 2), pAAV2-rtTA2s-S2-TRE-GDNF with Dox (lane 3), and pAAV2-rtTA2s-S2-TRE-GDNF without Dox (lane 4). (**c**) Dose–response of GDNF in the AAV2-S2-GDNF-injected muscle to the various concentrations of Dox. Mice were injected with phosphate-buffered saline (PBS), AAV2-LacZ, or AAV2-S2-GDNF followed by Dox administered in the drinking water. The mean muscle GDNF concentration in the animals treated with the AAV2-S2-GDNF in the absence of Dox was not significantly different compared to the animals treated with PBS or AAV2-*LacZ* ($P > 0.05$). The GDNF expression levels in the animals transduced with the AAV2-S2-GDNF significantly increased with increasing Dox concentration ($P < 0.05$). AAV1, adeno-associated virus 1.

In contrast, no detectable GDNF expression was observed in the cochlea of the AAV1-S2-GDNF/kanamycin group in the absence of Dox (data not shown).

Protection of cochlear function with induced GDNF expression

To evaluate the adverse effects of the transduction procedure, ABR recordings were performed on kanamycin-free rats after injection of the inducible AAV1-S2-GDNF vectors and Dox administration. At all frequencies tested, no significant increase in the ABR threshold was observed after virus injection (**Figure 8a**). This result indicates that AAV1 vector injection, transgene expression, and Dox administration did not affect the ABR threshold of the experimental rats. Interestingly, even if AAV1-S2-GDNF was injected into the cochlea of one ear, the cochleas of both ears were protected in the presence of Dox. In particular, the ABR threshold shifts were significantly improved in both the AAV1-S2-GDNF-injected cochlea of the kanamycin-treated rats in the presence of Dox (**Figure 8b**)

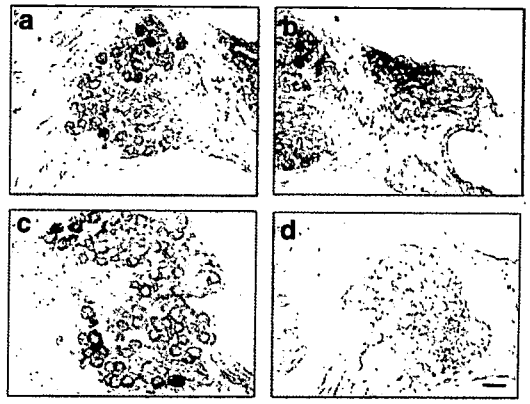

Figure 7 Expression of the GDNFflag in the rat cochlea. (**a**, **b**, **c**) The sections were sampled after the AAV1-S2-GDNF injection into the cochlea in the presence of doxycycline. GDNFflag expression was detected using an anti-FLAG antibody. (**d**) Samples from AAV1-EGFP-inoculated cochlea were analyzed as the negative control. Scale bar = 25 μm; ×400. AAV1, adeno-associated virus 1; GDNF, glial cell line–derived neurotrophic factor; EGFP, enhanced green fluorescent protein.

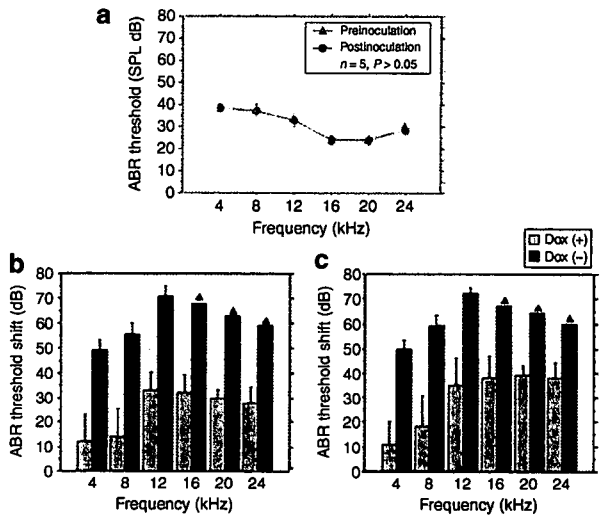

Figure 8 Protection of cochlear function with induced glial cell line–derived neurotrophic factor (GDNF) expression. (**a**) Auditory brain stem response (ABR) thresholds (mean ± SD) at each frequency tested in the AAV1-S2-GDNF-injected rat cochlea in the presence of doxycycline (Dox). No significant difference in the hearing thresholds was observed at each frequency between preinjection and postinjection. SPL, sound pressure level. ABR threshold shifts (mean ± SD) at each tested frequency in the (**b**) transduced or (**c**) nontransduced cochlea with or without Dox. Significant differences in the hearing threshold shifts were observed at each frequency between AAV1-S2-GDNF cochlea in the presence and absence of Dox ($n = 5$, $P < 0.05$). Arrows indicate the average ABR thresholds that exceeded the output power of the ABR apparatus.

and the cochlea of the noninjected contralateral ear (**Figure 8c**). However, the ABR threshold shifts at all frequencies were significantly lower in the treated group (AAV1-S2-GDNF/kanamycin plus Dox) than in the contralateral, untreated ear.

DISCUSSION

In this study, we showed that both sustained and regulated AAV1-mediated GDNF expression protected the cochlear function of rats from aminoglycoside-induced ototoxicity. Indeed, damaged spiral ganglion cells and hair cells were significantly reduced by

regulated GDNF expression. The ABR monitoring revealed that there was no loss of the cochlear function over the frequencies tested after AAV vector injection and Dox treatment. These data suggest that regulated expression of GDNF in the cochlea efficiently preserves the cochlea from kanamycin-induced ototoxicity.

Among the various viral vector systems, the recombinant AAV-mediated gene transduction system offers several important advantages as a tool for direct somatic gene delivery into the cochlea. These include long-term stable expression of therapeutic genes in a wide variety of postmitotic tissues and minimal vector-related cytotoxicity.[26] In our previous report, we demonstrated the effective transduction of mouse cochleae with the AAV1-based vectors.[7] Generally the therapeutic effectiveness depends on an appropriate concentration and the half-life of the molecules. AAV vector–mediated gene transfer is a promising delivery technique to facilitate a long-term and chronic supply of therapeutic proteins that have a short half-life, such as GDNF. Furthermore, when the CAG promoter is used, efficient transduction activity is observed in the cochlear cells including the inner hair cells and spiral ganglion cells.[27,28]

Our data showed that AAV1-GDNF-mediated transduction of the rat cochleae provided significant protection of the cochlea against aminoglycoside-induced damage. This finding is consistent with previous studies that have used adenovirus-mediated GDNF expression[13,15,16] and demonstrates the feasibility of gene therapy with AAV1-based vectors for drug-induced hearing loss. Although the exact mechanism has not yet been elucidated, antioxidant pathways might be involved in the protective function of GDNF in the inner ear.[29] Free-radical formation following exposure to aminoglycoside is considered one of the major mechanisms to explain the aminoglycoside-related hair cell death.[1,30,31] It has been previously shown that GDNF is endogenously synthesized in the inner hair cells and spiral ganglion cells of the cochlea,[32] and the two known GDNF receptors are present in the spiral ganglion.[17,32,33] In the present study, we inoculated the cochlea with the AAV1 vectors via the round window membrane and detected a high level of transgene expression mainly in the inner hair cells and spiral ganglion cells. The AAV1-mediated GDNF expression pattern was similar to that of the endogenous protein; therefore GDNF supplemented *in situ* can play a substantial role in protection. Although the transduction of the *GDNF* gene was not observed in outer hair cells, GDNF levels in the perilymph of the manipulated cochleae was much higher than in the control cochleae. These cells may respond to the secretion of another growth factor that promotes hair cell survival. Upregulation of GDNF in inner hair cells and spiral ganglion cells following noise also support this concept.[34]

Compared to the vehicle controls, increased cochlear cell survival was observed in the contralateral ears of the AAV1-GDNF group, suggesting that the contralateral cochleae in treated rats were also moderately protected. Expression of the transgene was detected in the contralateral cochlea of the rats after injection with 5×10^{10} genome copies of AAV1 per cochlea (data not shown). AAV can diffuse from one ear to the other via the cerebrospinal fluid in rodents.[35] Therefore, secreted GDNF molecules may also diffuse and exert a protective effect in the opposite ear. Alternatively, GDNF might enhance the neuronal activity (either afferent or efferent) of both ears, protecting both the treated and the contralateral cochlear function. Moreover, since infusion of the vectors into the cochlea forces large amounts of the vectors into the cerebrospinal fluid, any functional effect might be associated with the transduction of the brain. In this context, it is of great interest to know whether the otoprotective effect was achieved by the simple diffusion of the transgene product or direct transduction of the cells in the contralateral ear. To answer this question, we analyzed the local expression of the nonsecretory protein marker in the rodents with this transduction approach. Consequently, we feel that the direct transduction of the cells in the contralateral ear might be involved in the neuroprotection.

The present results showed that AAV-mediated delivery of a Tet-on system was able to control transgene expression. This Tet-on system incorporates the mutant transactivator rtTA2s-S2 and the transgene in which messenger RNA transcription is activated in the presence of an inducer, leading to protein expression. As we showed, the inducible expression of GDNF efficiently protected the cochlear structure and function from kanamycin-induced damage. GDNF was overexpressed in the induced state with the rtTA2s-S2 system, whereas GDNF expression was nearly normal in the non-induced state. In our study, cochlear function was significantly protected from aminoglycoside-induced cochlear damage in the presence of Dox. Although intracochlear injections did not affect physiological cochlear function, intramuscular injections of the vectors expressing Dox-dependent activators may elicit a cellular and humoral response against the transactivator in nonhuman primates.[36–38] The use of tissue-specific promoters that restrict transgene expression to nonprofessional antigen-presenting cells, and the use of AAV vectors, may reduce the induction of a specific T-cell response.[39]

Another attractive feature of the Tet-on system is the high safety profile of the inducer. In our study, Dox was orally administered to the rats to induce GDNF expression. Transgene expression levels were dependent on the dose of Dox, and the dose range of this inducer was below the normal bactericidal treatment levels used in similarly sized animals.[40,41] Furthermore, a Dox regimen in mice that is proportional to a clinically accepted dose of the drug in humans causes a significant induction of transgene expression.

Sequences of antibiotic administration and withdrawal to reverse the Dox induction of therapeutic gene expression were demonstrated in previous studies.[25,42] However, the aminoglycoside-induced hearing impairment model is not an appropriate model for adding and removing the Dox diet because the insulting phase is too short to successively induce and repress the Tet-on system. Furthermore, treatment of age-related hearing loss or genetic hearing loss ideally needs long-term gene expression studies to exclude any adverse events associated with the therapeutic genes.

Efficient control of the tetracycline-regulatory system is based on the specificity of the TetR/tetO interaction and the efficiency and safety of its inducers, such as tetracycline or Dox.[43,44] Mutant tTA2s are composed of one TetR and three repeated oligonucleotides of the VP-16-derived minimal activation domain. In the Tet-on system, rtTA2s-S2 showed a high activating ratio because its background expression level was lower than that of other mutants, such as rtTA2s-M2, which despite having a higher activation potential had also a high initial background.[25] By using the mutant transactivator, Urlinger *et al.* demonstrated that stringent regulation of target genes could be achieved over a range of four to five orders of magnitude

in stably transfected HeLa cells.[24] These regulatory systems could be further optimized to offer several potential advantages. The tetracycline-dependent transcriptional silencer allows tight regulation of transgene expression by eliminating baseline leakage.[20,45] Gene regulation mediated by rtTA2s-S2 was substantially tighter when combined with active silencing by the tetracycline-dependent transcriptional silencer in the non-induced state.[41,46]

Our results show that AAV1-mediated gene transfer is a promising gene delivery approach for the inner ear apparatus. To become an efficient and safe therapeutic method, it will be necessary to improve vector technology to achieve long-term transduction in a fail-safe system. We presented data demonstrating successful AAV-mediated transfer and modulation of transgene expression in the cochlea using a modified Tet-on system. In addition to the need for dosage control of neurotrophic factors, the AAV1 and the Tet-on system maybe useful for the regulation of the expression of other therapeutic gene products in the cochlea. Following further improvements, the rAAV-mediated transduction system may be of potential use for cochlear gene therapy applications in humans.

MATERIALS AND METHODS

Construction and preparation of the plasmids. The AAV vector proviral plasmid pAAV2-CAG-EGFP-WPRE (pAAV2-EGFP) contained the *EGFP* gene under the control of the CAG promoter and the WPRE and was flanked by inverted terminal repeats. A *Bam*HI fragment containing the GDNFflag complementary DNA was subcloned into this plasmid to obtain the pAAV2-CAG-GDNF-WPRE (pAAV2-GDNF) cassette.

The pAAV2-CMV-GDNFflag plasmid with the CMV promoter, the first intron of the human growth hormone gene, and the simian virus 40 polyadenylation signal sequence, were inserted between the inverted terminal repeats of the AAV type 2 genome.[47] The transactivator rtTA2s-S2 complementary DNA in the pUHrT61-1 plasmid (BD Biosciences, San Jose, CA) and the TRE in the pTRE-d2EGFP plasmid (BD Biosciences, CA) were subcloned together into the pAAV2-CMV-GDNFflag plasmid to obtain the AAV vector proviral plasmid pAAV2-rtTA2s-S2-TRE-GDNF. A *Sac*II-*Eco*RI fragment containing the d2EGFP complementary DNA from the pTRE-d2EGFP plasmid (BD Biosciences, CA) was subcloned into this plasmid to create the pAAV2-rtTA2s-S2-TRE-EGFP plasmid (see **Supplementary Materials and Methods**).

Recombinant AAV vector production. The AAV1 vectors were produced as previously described by using a 293-cell transfection protocol[26] with the proviral plasmid pAAV2-EGFP, pAAV2-Luciferase,[48] pAAV2-GDNF, pAAV2-rtTA2s-S2-TRE-EGFP, or pAAV2-rtTA2s-S2-TRE-GDNF; the AAV packaging plasmid pAAV1RepCap; and the adenovirus helper plasmid pAdeno5 using an active gassing system.[49] The recombinant AAV2 expressing the *Escherichia coli* β-galactosidase gene under the control of the CMV promoter (AAV2-LacZ) was generated using the proviral plasmid pAAV-LacZ.[50] (see **Supplementary Materials and Methods**).

In vitro *expression of GDNF.* To detect the *in vitro* expression of the GDNFflag fusion protein, 293 cells were transduced with the AAV1-GDNFflag at 1×10^4 vector genome copies/cell. For the detection of the regulated expression, 293 cells were transduced with the AAV proviral plasmid pAAV2-rtTA2s-S2-TRE-d2EGFP or pAAV2-rtTA2s-S2-TRE-GDNF in the presence or absence of 1 μmol/l Dox-HCl (Sigma, St Louis, MO) (see **Supplementary Materials and Methods**).

Surgical procedures and cochlear perfusions. All animal studies were performed in accordance with the guidelines issued by the committee on animal research at Jichi Medical University. Twenty 5-week-old male Sprague–Dawley rats with normal Preyer's reflexes weighing 130–150 g were utilized (CLEA Japan, Tokyo, Japan). Five-week-old male C57BL/6J mice were utilized for optical bioluminescence imaging. The animals were anesthetized with ketamine (50 mg/kg) and xylazine (5 mg/kg). A postauricular approach was performed to expose the tympanic bony bulla. A small opening (2 mm in diameter) to the tympanic bulla was made by carefully drilling through the bone of the bulla to gain access to the round window membrane. Subsequently, 5 μl of AAV vector solution (AAV1-EGFP, AAV2-Luciferase, or AAV1-GDNF, 5×10^{10} genome copies, $n = 5$ each) was microinjected into the cochlea through the round window for over 10 minutes using a glass micropipette (40 μm in diameter) fitted on a Univentor 801 syringe pump (Serial No. 170182, High Precision Instruments, Univentor Ltd., Malta). The rats were also injected with the AAV1-S2-GDNF in the presence ($n = 5$) or absence ($n = 5$) of Dox. A small plug of muscle was used to seal the cochlea, and the surgical wound was closed in layers and dressed with an antibiotic ointment.

***Transgene expression* in vivo.** The rats were deeply anesthetized and the perilymph was sampled from the inoculated cochlea through the round window. GDNF protein levels were measured using a GDNF Emax ImmunoAssay System (Promega, Madison, WI) according to the manufacturer's instructions. The GDNF expression in the rat cochlea was determined by immunohistochemistry using an anti-FLAG antibody.

AAV2-LacZ or AAV2-S2-GDNF vector (1×10^{10} genome copies) was injected into the quadriceps of the C57BL/6J mice (6 weeks old, CLEA Japan, Tokyo, Japan). The mice were injected with phosphate-buffered saline ($n = 5$) or AAV2-*LacZ* ($n = 5$). Animals treated with various concentrations of Dox were injected with the AAV2-S2-GDNF ($n = 5$ per group). Two weeks after the transduction, animals were deeply anesthetized, and the injected muscle was sampled. The tissue levels of the GDNF protein were measured with an enzyme-linked immunosorbent assay kit (GDNF Emax ImmunoAssay System, Promega, WI), according to the manufacturer's instructions. The levels of GDNF were expressed as pg/mg protein. The assay sensitivity ranged from 16 to 1,000 pg/ml.

Two weeks after the injection of the AAV2-Luciferase, optical bioluminescence imaging was performed using the CCD camera (Xenogen, Alameda, CA). After intraperitoneal injection of reporter substrate D-Luciferin (375 mg/kg body weight), mice were imaged for scans.

Kanamycin administration and ABR assessment. A dose of 333 mg of kanamycin base/kg body weight was obtained by injecting 3 μl/g body weight. Seven days after virus injection, kanamycin was given subcutaneously twice daily for 12 consecutive days. The body weight of the animals was monitored daily to adjust the kanamycin dosages accordingly.

Auditory thresholds were determined by audiometry of evoked ABRs using Tucker-DAVIS Technologies and Scope software (Power Lab; ADInstruments, Coloado Springs, CO). Thresholds were evaluated for each animal prior to the start of the injection procedure and 2 days after the termination of kanamycin treatment. The ABRs were measured as previously described,[7] using a two-way repeated analysis of variance (see **Supplementary Materials and Methods**).

Histological evaluation of the cochlear preservation. Cochlear hair cell loss was determined by F-actin staining. One month after transduction, the presence of the cochlear spiral ganglion neurons was determined by 4′,6-diamino-2-phenylindole dihydrochloride staining to visualize nuclear chromatin. After decalcification, 6 μm mid-modiolus cryosections of the cochleae from each animal were histologically analyzed. The number of spiral ganglion neurons was determined in every third section of the cochlear basal turn from the AAV1-transduced and kanamycin-treated rats (see **Supplementary Materials and Methods**).

Statistical analyses. Results are presented as the means ± SD. Data were statistically analyzed using analysis of variance, paired student's *t*-test (injected versus contralateral sides) or unpaired student's *t*-test (therapy versus control groups) (StatView 5.0 software; SAS Institute, Cary, NC).

ACKNOWLEDGMENTS

The authors thank Avigen. (Alameda, CA) for providing the pAAV-LacZ and pAdeno. We also thank Thomas Hope (Department of Microbiology and Immunology, The University of Illinois at Chicago) for providing pBS II SK+WPRE-B11 and Jun-Ichi Miyazaki (Osaka University Graduate School of Medicine, Osaka, Japan) for pCAGGS. The authors also thank Miyoko Mitsu for her encouragement and technical support. This work was supported in part by grants from the Ministry of Health, Labour and Welfare of Japan (Grants-in-Aid for Scientific Research and grant for 21 Century Centers of Excellence program) and the "High-Tech Research Center" Project for Private Universities (matching fund subsidy, from the Ministry of Education, Culture, Sports, Science, and Technology of Japan). The authors declare no conflict of interest.

SUPPLEMENTARY MATERIAL

Materials and Methods.

Figure S1. Bioluminescence of the transduced cochlea in living mice.

REFERENCES

1. Wu, WJ, Sha, SH and Schacht, J (2002). Recent advances in understanding aminoglycoside ototoxicity and its prevention. *Audiol Neurootol* **7**: 171–174.
2. Hellier, WP, Wagstaff, SA, O'Leary, SJ and Shepherd, RK (2002). Functional and morphological response of the stria vascularis following a sensorineural hearing loss. *Hear Res* **172**: 127–136.
3. Tsue, TT, Oesterle, EC and Rubel, EW (1994). Hair cell regeneration in the inner ear. *Otolaryngol Head Neck Surg* **111**: 281–301.
4. Raphael, Y, Frisancho, JC and Roessler, BJ (1996). Adenoviral-mediated gene transfer into guinea pig cochlear cells *in vivo*. *Neurosci Lett* **207**: 137–141.
5. Ishimoto, S, Kawamoto, K, Kanzaki, S and Raphael, Y (2002). Gene transfer into supporting cells of the organ of Corti. *Hear Res* **173**: 187–197.
6. Okada, T, Nomoto, T, Shimazaki, K, Lijun, W, Lu, Y, Matsushita, T *et al.* (2002). Adeno-associated virus vectors for gene transfer to the brain. *Methods* **28**: 237–247.
7. Liu, Y, Okada, T, Sheykholeslami, K, Shimazaki, K, Nomoto, T, Muramatsu, SI *et al.* (2005). Specific and efficient transduction of cochlear inner hair cells with recombinant adeno-associated virus type 3 vector. *Mol Ther* **12**: 725–733.
8. Lin, LF, Doherty, DH, Lile, JD, Bektesh, S and Collins, F (1993). GDNF: a glial cell line-derived neurotrophic factor for midbrain dopaminergic neurons. *Science* **260**: 1130–1132.
9. Henderson, CE, Phillips, HS, Pollock, RA, Davies, AM, Lemeulle, C, Armanini, M *et al.* (1994). GDNF: a potent survival factor for motoneurons present in peripheral nerve and muscle. *Science* **266**: 1062–1064.
10. Wang, Y, Lin, SZ, Chiou, AL, Williams, LR and Hoffer, BJ (1997). Glial cell line-derived neurotrophic factor protects against ischemia-induced injury in the cerebral cortex. *J Neurosci* **17**: 4341–4348.
11. Keithley, EM, Ma, CL, Ryan, AF, Louis, JC and Magal, E (1998). GDNF protects the cochlea against noise damage. *Neuroreport* **9**: 2183–2187.
12. Shoji, F, Yamasoba, T, Magal, E, Dolan, DF, Altschuler, RA and Miller, JM (2000). Glial cell line-derived neurotrophic factor has a dose dependent influence on noise-induced hearing loss in the guinea pig cochlea. *Hear Res* **142**: 41–55.
13. Suzuki, M, Yagi, M, Brown, JN, Miller, AL, Miller, JM and Raphael, Y (2000). Effect of transgenic GDNF expression on gentamicin-induced cochlear and vestibular toxicity. *Gene Ther* **7**: 1046–1054.
14. Yagi, M, Kanzaki, S, Kawamoto, K, Shin, B, Shah, PP, Magal, E *et al.* (2000). Spiral ganglion neurons are protected from degeneration by GDNF gene therapy. *J Assoc Res Otolaryngol* **1**: 315–325.
15. Hakuba, N, Watabe, K, Hyodo, J, Ohashi, T, Eto, Y, Taniguchi, M *et al.* (2003). Adenovirus-mediated overexpression of a gene prevents hearing loss and progressive inner hair cell loss after transient cochlear ischemia in gerbils. *Gene Ther* **10**: 426–433.
16. Kawamoto, K, Yagi, M, Stover, T, Kanzaki, S and Raphael, Y (2003). Hearing and hair cells are protected by adenoviral gene therapy with TGF-beta1 and GDNF. *Mol Ther* **7**: 484–492.
17. Kuang, R, Hever, G, Zajic, G, Yan, Q, Collins, F, Louis, JC *et al.* (1999). Glial cell line-derived neurotrophic factor. Potential for otoprotection. *Ann NY Acad Sci* **884**: 270–291.
18. Yagi, M, Magal, E, Sheng, Z, Ang, KA and Raphael, Y (1999). Hair cell protection from aminoglycoside ototoxicity by adenovirus-mediated overexpression of glial cell line-derived neurotrophic factor. *Hum Gene Ther* **10**: 813–823.
19. Meng, X, Lindahl, M, Hyvonen, ME, Parvinen, M, de Rooij, DG, Hess, MW *et al.* (2000). Regulation of cell fate decision of undifferentiated spermatogonia by GDNF. *Science* **287**: 1489–1493.
20. Perez, N, Plence, P, Millet, V, Greuet, D, Minot, C, Noel, D *et al.* (2002). Tetracycline transcriptional silencer tightly controls transgene expression after *in vivo* intramuscular electrotransfer: application to interleukin 10 therapy in experimental arthritis. *Hum Gene Ther* **13**: 2161–2172.
21. Regulier, E, Pereira de Almeida, L, Sommer, B, Aebischer, P and Deglon, N (2002). Dose-dependent neuroprotective effect of ciliary neurotrophic factor delivered via tetracycline-regulated lentiviral vectors in the quinolinic acid rat model of Huntington's disease. *Hum Gene Ther* **13**: 1981–1990.
22. Rubinchik, S, Woraratanadharm, J, Yu, H and Dong, JY (2005). New complex Ad vectors incorporating both rtTA and tTS deliver tightly regulated transgene expression both *in vitro* and *in vivo*. *Gene Ther* **12**: 504–511.
23. Pluta, K, Luce, MJ, Bao, L, Agha-Mohammadi, S and Reiser, J (2005). Tight control of transgene expression by lentivirus vectors containing second-generation tetracycline-responsive promoters. *J Gene Med* **7**: 803–817.
24. Urlinger, S, Baron, U, Thellmann, M, Hasan, MT, Bujard, H and Hillen, W (2000). Exploring the sequence space for tetracycline-dependent transcriptional activators: novel mutations yield expanded range and sensitivity. *Proc Natl Acad Sci USA* **97**: 7963–7968.
25. Lamartina, S, Roscilli, G, Rinaudo, CD, Sporeno, E, Silvi, L, Hillen, W *et al.* (2002). Stringent control of gene expression *in vivo* by using novel doxycycline-dependent trans-activators. *Hum Gene Ther* **13**: 199–210.
26. Okada, T, Shimazaki, K, Nomoto, T, Matsushita, T, Mizukami, H, Urabe, M *et al.* (2002). Adeno-associated viral vector-mediated gene therapy of ischemia-induced neuronal death. *Methods Enzymol* **346**: 378–393.
27. Stone, IM, Lurie, DI, Kelley, MW and Poulsen, DJ (2005). Adeno-associated virus-mediated gene transfer to hair cells and support cells of the murine cochlea. *Mol Ther* **11**: 843–848.
28. Liu, Y, Okada, T, Nomoto, T, Ke, X, Kume, A, Ozawa, K *et al.* (2007). Promoter effects of adeno-associated viral vector for transgene expression in the cochlea *in vivo*. *Exp Mol Med* **39**: 170–175.
29. Oppenheim, RW (1997). Related mechanisms of action of growth factors and antioxidants in apoptosis: an overview. *Adv Neurol* **72**: 69–78.
30. Priuska, EM and Schacht, J (1995). Formation of free radicals by gentamicin and iron and evidence for an iron/gentamicin complex. *Biochem Pharmacol* **50**: 1749–1752.
31. Sha, SH and Schacht, J (1999). Stimulation of free radical formation by aminoglycoside antibiotics. *Hear Res* **128**: 112–118.
32. Sanicola, M, Hession, C, Worley, D, Carmillo, P, Ehrenfels, C, Walus, L *et al.* (1997). Glial cell line-derived neurotrophic factor-dependent RET activation can be mediated by two different cell-surface accessory proteins. *Proc Natl Acad Sci USA* **94**: 6238–6243.
33. Ylikoski, J, Pirvola, U, Virkkala, J, Suvanto, P, Liang, XQ, Magal, E *et al.* (1998). Guinea pig auditory neurons are protected by glial cell line-derived growth factor from degeneration after noise trauma. *Hear Res* **124**: 17–26.
34. Nam, YJ, Stover, T, Hartman, SS and Altschuler, RA (2000). Upregulation of glial cell line-derived neurotrophic factor (GDNF) in the rat cochlea following noise. *Hear Res* **146**: 1–6.
35. Kho, ST, Pettis, RM, Mhatre, AN and Lalwani, AK (2000). Safety of adeno-associated virus as cochlear gene transfer vector: analysis of distant spread beyond injected cochleae. *Mol Ther* **2**: 368–373.
36. Favre, D, Blouin, V, Provost, N, Spisek, R, Porrot, F, Bohl, D *et al.* (2002). Lack of an immune response against the tetracycline-dependent transactivator correlates with long-term doxycycline-regulated transgene expression in non-human primates after intramuscular injection of recombinant adeno-associated virus. *J Virol* **76**: 11605–11611.
37. Latta-Mahieu, M, Rolland, M, Caillet, C, Wang, M, Kennel, P, Mahfouz, I *et al.* (2002). Gene transfer of a chimeric trans-activator is immunogenic and results in short-lived transgene expression. *Hum Gene Ther* **13**: 1611–1620.
38. Lena, AM, Giannetti, P, Sporeno, E, Ciliberto, G and Savino, R (2005). Immune responses against tetracycline-dependent transactivators affect long-term expression of mouse erythropoietin delivered by a helper-dependent adenoviral vector. *J Gene Med* **7**: 1086–1096.
39. Cordier, L, Gao, GP, Hack, AA, McNally, EM, Wilson, JM, Chirmule, N *et al.* (2001). Muscle-specific promoters may be necessary for adeno-associated virus-mediated gene transfer in the treatment of muscular dystrophies. *Hum Gene Ther* **12**: 205–215.
40. McGee Sanftner, LH, Rendahl, KG, Quiroz, D, Coyne, M, Ladner, M, Manning, WC *et al.* (2001). Recombinant AAV-mediated delivery of a tet-inducible reporter gene to the rat retina. *Mol Ther* **3**: 688–696.
41. Lamartina, S, Silvi, L, Roscilli, G, Casimiro, D, Simon, AJ, Davies, ME *et al.* (2003). Construction of an rtTA2(s)-m2/tts(kid)-based transcription regulatory switch that displays no basal activity, good inducibility, and high responsiveness to doxycycline in mice and non-human primates. *Mol Ther* **7**: 271–280.
42. Srour, MA, Fechner, H, Wang, X, Siemetzki, U, Albert, T, Oldenburg, J *et al.* (2003). Regulation of human factor IX expression using doxycycline-inducible gene expression system. *Thromb Haemost* **90**: 398–405.
43. Kistner, A, Gossen, M, Zimmermann, F, Jerecic, J, Ullmer, C, Lubbert, H *et al.* (1996). Doxycycline-mediated quantitative and tissue-specific control of gene expression in transgenic mice. *Proc Natl Acad Sci USA* **93**: 10933–10938.
44. Knott, A, Garke, K, Urlinger, S, Guthmann, J, Muller, Y, Thellmann, M *et al.* (2002). Tetracycline-dependent gene regulation: combinations of transregulators yield a variety of expression windows. *Biotechniques* **32**: 796, 798, 800 passim.
45. Rendahl, KG, Quiroz, D, Ladner, M, Coyne, M, Seltzer, J, Manning, WC *et al.* (2002). Tightly regulated long-term erythropoietin expression in vivo using tet-inducible recombinant adeno-associated viral vectors. *Hum Gene Ther* **13**: 335–342.
46. Salucci, V, Scarito, A, Aurisicchio, L, Lamartina, S, Nicolaus, G, Giampaoli, S *et al.* (2002). Tight control of gene expression by a helper-dependent adenovirus vector carrying the rtTA2(s)-M2 tetracycline transactivator and repressor system. *Gene Ther* **9**: 1415–1421.
47. Wang, L, Muramatsu, S, Lu, Y, Ikeguchi, K, Fujimoto, K, Okada, T *et al.* (2002). Delayed delivery of AAV-GDNF prevents nigral neurodegeneration and promotes functional recovery in a rat model of Parkinson's disease. *Gene Ther* **9**: 381–389.
48. Okada, T, Uchibori, R, Iwata-Okada, M, Takahashi, M, Nomoto, T, Nonaka-Sarukawa, M *et al.* (2006). A histone deacetylase inhibitor enhances recombinant adeno-associated virus-mediated gene expression in tumor cells. *Mol Ther* **13**: 738–746.
49. Okada, T, Nomoto, T, Yoshioka, T, Nonaka-Sarukawa, M, Ito, T, Ogura, T *et al.* (2005). Large-scale production of recombinant viruses by use of a large culture vessel with active gassing. *Hum Gene Ther* **16**: 1212–1218.
50. Okada, T, Mizukami, H, Urabe, M, Nomoto, T, Matsushita, T, Hanazono, Y *et al.* (2001). Development and characterization of an antisense-mediated prepackaging cell line for adeno-associated virus vector production. *Biochem Biophys Res Commun* **288**: 62–68.

Interleukin-10 Expression Mediated by an Adeno-Associated Virus Vector Prevents Monocrotaline-Induced Pulmonary Arterial Hypertension in Rats

Takayuki Ito, Takashi Okada, Hiroshi Miyashita, Tatsuya Nomoto, Mutsuko Nonaka-Sarukawa, Ryosuke Uchibori, Yoshikazu Maeda, Masashi Urabe, Hiroaki Mizukami, Akihiro Kume, Masafumi Takahashi, Uichi Ikeda, Kazuyuki Shimada, Keiya Ozawa

Abstract—Pulmonary arterial hypertension (PAH) is a fatal disease associated with inflammation and pathological remodeling of the pulmonary artery (PA). Interleukin (IL)-10 is a pleiotropic antiinflammatory cytokine with vasculoprotective properties. Here, we report the preventive effects of IL-10 on monocrotaline-induced PAH. Three-week-old Wistar rats were intramuscularly injected with an adeno-associated virus serotype 1 vector expressing IL-10, followed by monocrotaline injection at 7 weeks old. IL-10 transduction significantly improved survival rates of the PAH rats 8 weeks after monocrotaline administration compared with control gene transduction (75% versus 0%, $P<0.01$). IL-10 also significantly reduced mean PA pressure (22.8±1.5 versus 29.7±2.8 mm Hg, $P<0.05$), a weight ratio of right ventricle to left ventricle plus septum (0.35±0.04 versus 0.42±0.05, $P<0.05$), and percent medial thickness of the PA (12.9±0.3% versus 21.4±0.4%, $P<0.01$) compared with controls. IL-10 significantly reduced macrophage infiltration and vascular cell proliferation in the remodeled PA in vivo. It also significantly decreased the lung levels of transforming growth factor-β_1 and IL-6, which are indicative of PA remodeling. In addition, IL-10 increased the lung level of heme oxygenase-1, which strongly prevents PA remodeling. In vitro analysis revealed that IL-10 significantly inhibited excessive proliferation of cultured human PA smooth muscle cells treated with transforming growth factor-β_1 or the heme oxygenase inhibitor tin protoporphyrin IX. Thus, IL-10 prevented the development of monocrotaline-induced PAH, and these results provide new insights into the molecular mechanisms of human PAH. (*Circ Res.* 2007;101:734-741.)

Key Words: pulmonary hypertension ■ interleukins ■ gene therapy ■ inflammation ■ vascular smooth muscle cell proliferation

Pulmonary arterial hypertension (PAH) is an intractable disease that leads to increased pulmonary arterial pressure, progressive right heart failure, and premature death; however, no satisfactory treatment for PAH has been established.[1] The pathological process of PAH is characterized by abnormal remodeling of the pulmonary artery (PA) associated with excessive proliferation of pulmonary arterial smooth muscle cells (PASMCs).[2] Accumulating evidence suggests important roles of vascular inflammation in its pathogenesis.[2,3] For instance, serum levels of proinflammatory cytokines such as interleukin (IL)-1 and IL-6 reflect the disease activity in patients with idiopathic PAH.[4] Furthermore, injection of IL-6 can produce PAH and PA remodeling in rats.[5] The remodeled PA presents macrophage infiltration and increased expression of a variety of cytokines, including IL-6, tumor necrosis factor (TNF)-α, and transforming growth factor (TGF)-β_1.[6,7] Administration of steroids or immunosuppressive drugs decreases the level of PA pressure in patients with PAH.[8,9] These observations suggest a therapeutic potential of targeting inflammation to prevent PAH progression.[10] However, the precise mechanisms underlying the antiinflammatory effects on PA remodeling have not yet been fully investigated.

IL-10 is a multifunctional antiinflammatory cytokine with a vasculoprotective property. During the course of inflammation, IL-10 is produced by type-2 helper T (Th2) lymphocytes, and it inhibits the production of various proinflammatory cytokines in macrophages and Th1 lymphocytes.[11] Exogenous IL-10 prevents proliferative vasculopathy in vivo by inhibiting inflammatory cell infiltration,[12] smooth muscle cell proliferation,[12,13] and chemokine expression.[14] However, clinical efficacy of systemic recombinant IL-10 administra-

Original received March 28, 2007; revision received July 12, 2007; accepted July 23, 2007.

From the Division of Genetic Therapeutics (T.I., T.N., M.N.-S., M.U., H.M., A.K., K.O., R.U.), the Division of Cardiovascular Medicine (T.I., H.M., M.N.-S., K.S., Y.M.), Jichi Medical University, Japan; the Department of Molecular Therapy (T.O.), National Institute of Neuroscience, National Center of Neurology and Psychiatry, Japan; and the Department of Organ Regeneration (M.T., U.I.), Shinshu University Graduate School of Medicine, Japan.

Correspondence to Takayuki Ito, MD, PhD, Division of Genetic Therapeutics, Jichi Medical University, 3311-1 Yakushiji, Shimotsuke, Tochigi 329-0498, Japan. E-mail titou@jichi.ac.jp

Circulation Research is available at http://circres.ahajournals.org DOI: 10.1161/CIRCRESAHA.107.153023

tion are insufficient because of the lower local IL-10 levels resulting from its short bioactive half-life.[15] In this study, we used an adeno-associated virus (AAV) vector for IL-10 expression because it is an efficient vehicle for systemic and sustained expression of therapeutic proteins.[14] It also has an advantage over other viral vectors in the therapeutic or mechanistic analysis because it produces minimal inflammatory and immune responses in vivo.

Recently, heme oxygenase (HO)-1, an inducible form of HO that promotes production of a vasodilator carbon monoxide (CO), was shown to mediate antiinflammatory and antiproliferative effects of IL-10 in a model of chronic vasculopathy.[12] Increased HO-1 and CO levels attenuated PAH and PA remodeling by inhibiting PASMC proliferation.[16–18] However, no study has explored a direct link between IL-10 and HO-1 in the pathogenesis of PAH. Thus, we examined the effects of IL-10, delivered via an AAV vector, on PA remodeling in a widely-used rat model of PAH induced by the pyrolizidine alkaloid monocrotaline (MCT). We also investigated the mechanisms underlying the effects of IL-10 on the following factors involved in the inflammatory and proliferative vascular changes in PAH: PASMC, macrophage, TGF-β_1, IL-6, and HO-1.

Materials and Methods

AAV Vector Production

DNA encoding rat IL-10 was polymerase chain reaction-amplified from rat splenocyte complementary DNA, using the primers 5′-GCACGAGAGCCACAACGCA-3′ and 5′-GATTTGAGTACG-ATCCATTTATTCAAAACGAGGAT-3′. For efficient transgene expression in the skeletal muscle, we constructed a recombinant AAV vector which carried the IL-10 gene (AAV-IL-10) or enhanced green fluorescent protein (eGFP) gene (AAV-eGFP), controlled by the modified chicken β-actin promoter with the cytomegalo virus-immediate early enhancer and the woodchuck hepatitis virus post-transcriptional regulatory element (a kind gift from Dr Thomas Hope, Infectious Disease Laboratory, Salk Institute). AAV vectors were prepared according to the previously described 3-plasmid transfection adenovirus-free protocol with minor modifications to use the active gassing system.[19,20] In brief, 60% confluent human embryonic kidney 293 cells incubated in a large culture vessel with active air circulation were cotransfected with the proviral transgene plasmid, AAV-1 chimeric helper plasmid (p1RepCap), and adenoviral helper plasmid pAdeno (Avigen Inc). The crude viral lysate was purified by 2 rounds of cesium chloride 2-tier centrifugation.[21] The viral stock titer was determined against plasmid standards by dot blot hybridization, after which the stock was dissolved in HN buffer (50 mmol/L HEPES, pH 7.4, 0.15 mol/L NaCl) before injection.

Animal Models

All animal experiments were approved by the Jichi Medical University ethics committee and were performed in accordance with the *National Institute of Health Guide for the Care and Use of Laboratory Animals*. To evaluate the efficiency of in vivo gene expression, 3-week-old male Wistar rats (Clea Japan Inc, Tokyo, Japan) weighing 45 to 55 g were injected with AAV-IL-10 (200 μL, 3×10^{10} to 1×10^{11} genome copies [g.c.] per body) into the bilateral anterior tibial muscles (n=3 animals per group). For hemodynamic and histological analysis, we randomly formed 4 groups comprising 5 rats each: sham rats that were administered the HN buffer (1, NC group); MCT-treated rats administered the HN buffer (2, MCT group); MCT rats administered AAV-eGFP (3, MCT+eGFP group); and MCT rats administered AAV-IL-10 (4, MCT+IL-10 group). After anesthetized with a spontaneous inhalation of 1% isoflurane, the rats in the groups 3 and 4 received intramuscular injection of AAV-eGFP or AAV-IL-10 (200 μL, 6×10^{10} g.c. per body), respectively. Rats in groups 1 and 2 were injected with the HN buffer (200 μL). MCT (Wako Pure Chemicals) was dissolved in 0.1N HCl, and the pH adjusted to 7.4 with 1.0N NaOH. For hemodynamic and histological studies, all rats except those in the NC group were subcutaneously injected with MCT (30 mg/kg) under the spontaneous inhalation of 1% isoflurane at 4 weeks after vector treatment. For the survival study, rats (n=8 animals/group) were injected with a lethal dose of MCT (45 mg/kg) under the spontaneous inhalation of 1% isoflurane at 4 weeks after vector injection. Survival was estimated from the date of MCT injection until death or 8 weeks after injection.

Hemodynamic Analysis

Four weeks after MCT injection, the rats were anesthetized with spontaneous inhalation of 1% isoflurane, and a tracheotomy was performed. Then, they were mechanically ventilated using a respirator (SAR-830/AP, CWE; tidal volume: 10 mL/kg, respiratory rate: 30 breaths per min) and anesthetized with 0.5% isoflurane through a tracheostomy. After the thoracic cavity was opened using a midsternal approach, 2.0F high-fidelity manometer-tipped catheters (SPC-320, Millar Instruments Inc) were inserted directly into the right or left ventricle. The mean pulmonary arterial pressure (mPAP) or mean aortic arterial pressure (mAoP) was measured using the catheters that were advanced from the right or left ventricle, respectively. The heart rate (HR) was measured by unipolar lead electrocardiography.

Ventricular Weight Measurement and Morphometric Analysis of the PA

After hemodynamic analysis, the rats were euthanized using an overdose isoflurane (5%). The lungs and PAs were perfused with 5 mL of saline followed by 10 mL of cold 4% paraformaldehyde. Each ventricle and the lungs were excised, dissected free, and weighed. The weight ratio of right ventricle to the left ventricle plus septum [RV/(LV+S)] was calculated as an index of right ventricular hypertrophy (RVH). The tissues were fixed in 4% paraformaldehyde for 4 hours, transferred to 30% sucrose in 0.1 mol/L phosphate buffer (pH 7.4) for cryoprotection, and stored at 4°C overnight. Lung tissue was frozen in Tissue-Tek OCT compound (Sakura Finetechnical Co) at −20°C. Then, 7-μm sections were cut using a cryostat. Hematoxylin and eosin (HE) staining was performed on sections from the middle lobe of the right lung, and these were examined using light microscopy. Morphometric analysis was performed in PAs with an external diameter of 25 to 50 and 51 to 100 μm. The medial wall thickness was calculated with the following formula: medial thickness (%)=medial wall thickness/external diameter×100.[22] For quantitative analysis, 30 vessels from each rat were counted and the average was calculated.

Immunohistochemistry

Immunohistochemical staining was performed with monoclonal antibodies against ED1 (1:100; Serotec) and proliferating cell nuclear antigen (PCNA, 1:200; Zymed), using the streptavidin-biotin-peroxidase method, as described previously.[23] ED1 recognizes the lysosomal membrane antigen expressed by a majority of tissue macrophages. Irrelevant mouse immunoglobulin G (Vector Laboratories) was used as a negative control. Reactions were visualized using Vector SG (Vector Laboratories) or 3,3′-diaminobenzidine (Zymed) and counterstained with nuclear fast red or hematoxylin. The number of ED1-positive cells was counted in 250×250-μm fields under 400× magnification and expressed as cells per mm^2. The number of PCNA-positive cells was quantitatively evaluated as a percentage of total vascular cells in the fields under 1000× magnification. For each rat, the average number or percentage of each cell in 15 randomly selected fields was used for statistical analysis.

Protein Assay

Protein samples were prepared by homogenization of the frozen lung tissue in lysis buffer [10 μmol/L Tris/Cl (pH 8.0), 0.2% NP-40,